

Integration of Geophysical and Geomechanical Modeling to Monitor Integrity of Carbon Storage



gemlab.usc.edu

Birendra Jha

Assistant Professor

Department of Chemical engineering and Materials Science

University of Southern California

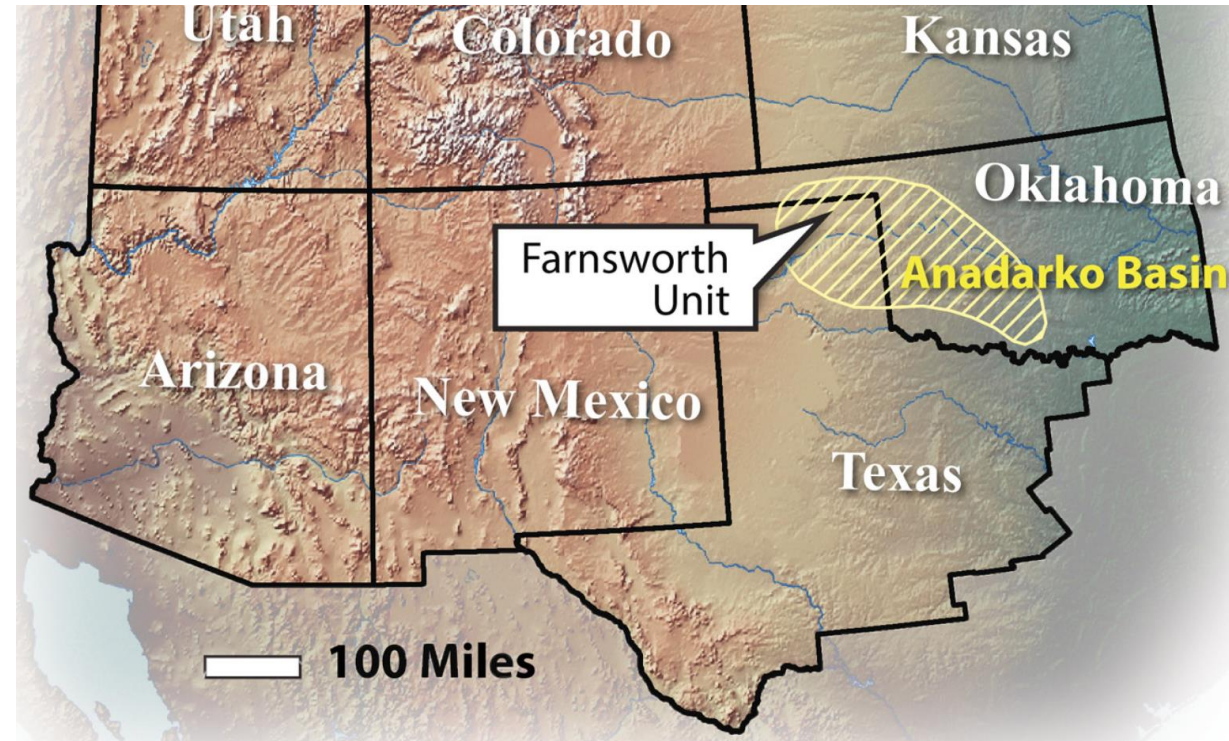
Case study: CO₂-EOR in Farnsworth Unit

Integration of three technologies

- Coupled flow and geomechanical modeling (field scale)
- New seismic imaging techniques and attributes (well scale)
- Experimental characterization of CO₂-induced changes in rock mechanical properties (nano, micro, core scale)

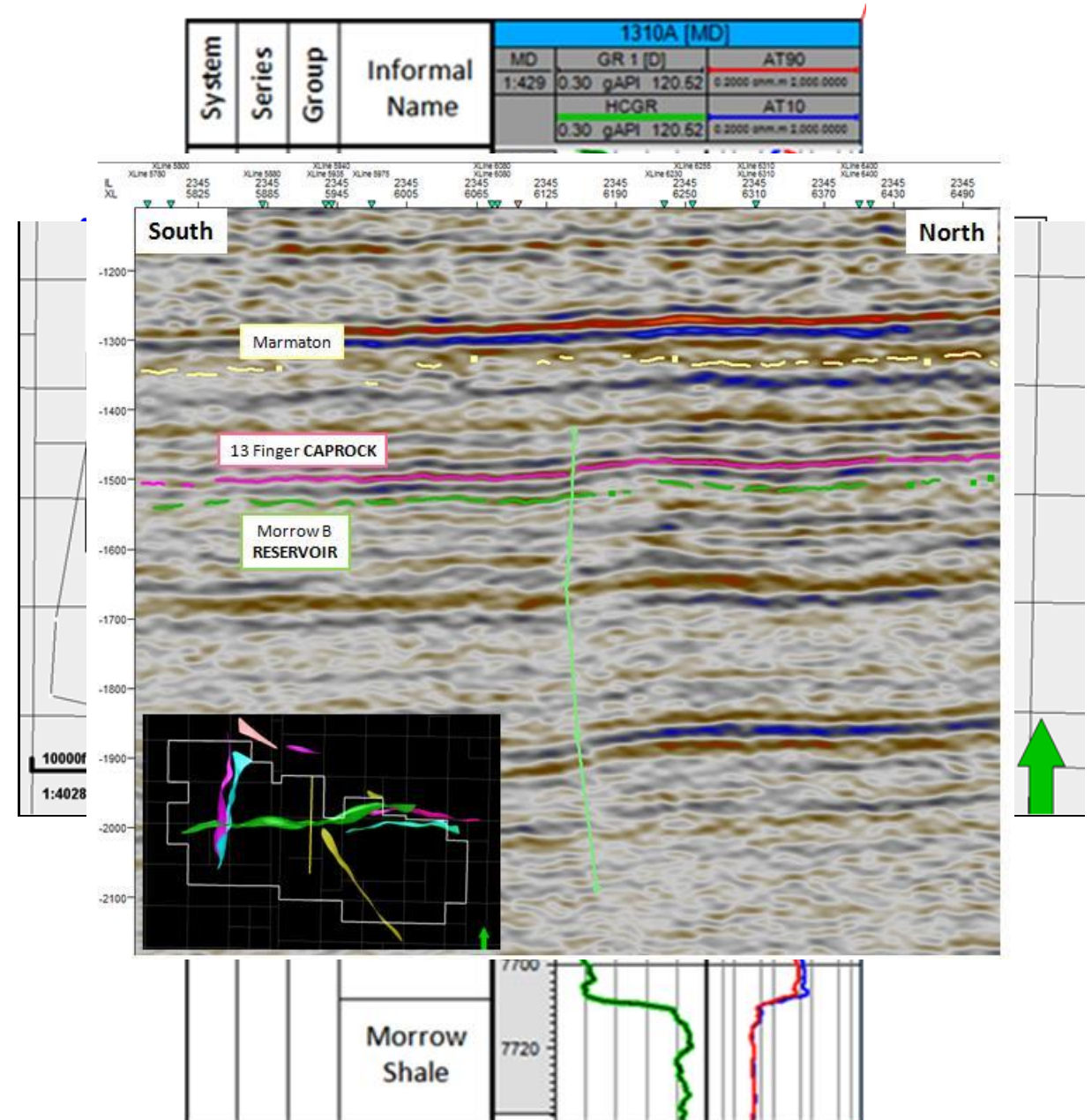
Farnsworth Unit (FWU) oilfield, Texas

- Southwest Regional Partnership on Carbon Sequestration (SWP), established in 2003 by DOE
- Active oil field with 19 million barrel oil produced under primary recovery, waterflood and CO₂ EOR
- CO₂ storage is a part of EOR
- CO₂ storage capacity of 25 million metric ton
- 76 wells, 13 CO₂ injection wells
- 1 million metric ton of CO₂ injected
- CO₂ from a fertilizer plant in Texas and an ethanol plant in Kansas



Farnsworth Unit (FWU)

- Well locations by drilling year
- Production and injection from Morrow-B sandstone
- Morrow Shale and Thirteen Finger Limestone are the caprocks
- Nine faults are interpreted from 3-D surface seismic
- Fault-1 dips 6° to the west
- Fault-3 dips 6° to the north

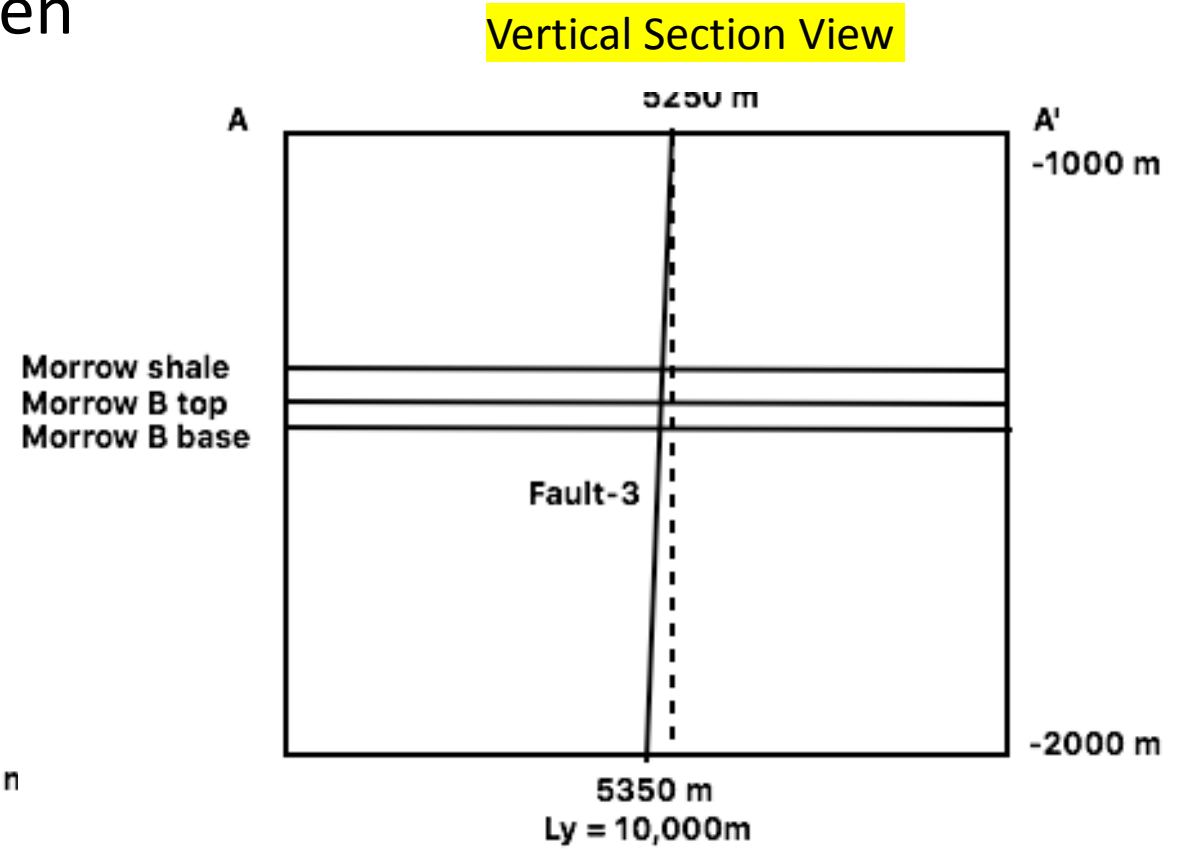
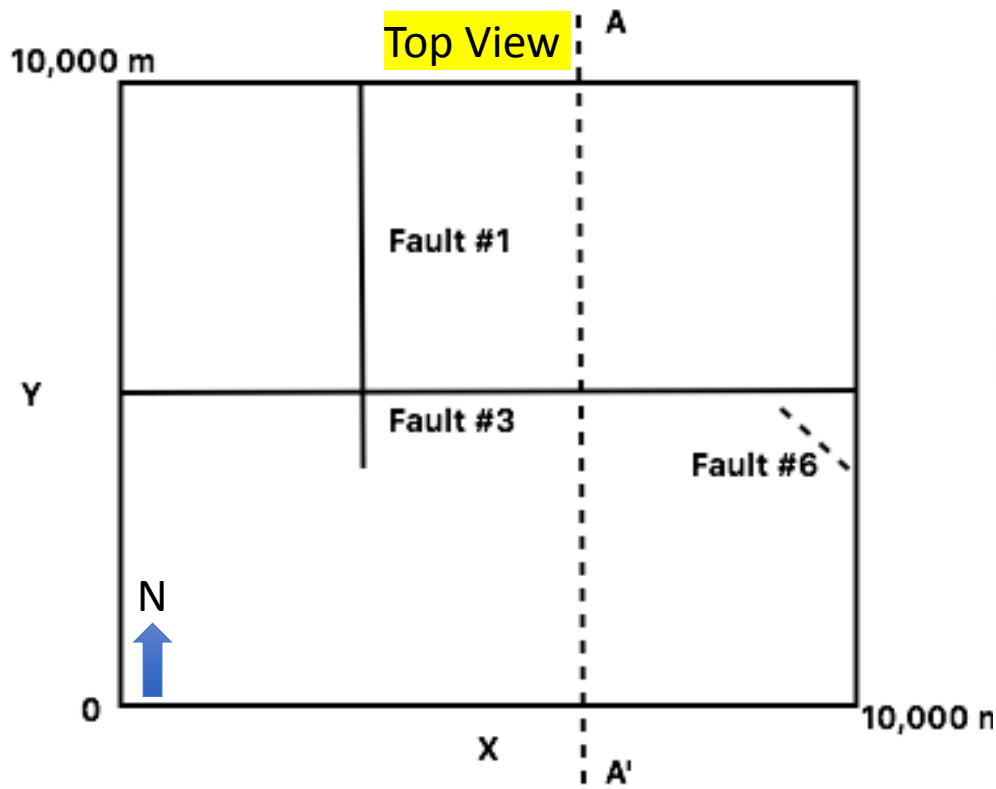


Coupled Flow and Geomechanical Simulation

Objective: Model the CO₂-induced changes in pressure, saturation and stress in the CO₂ storage-EOR system

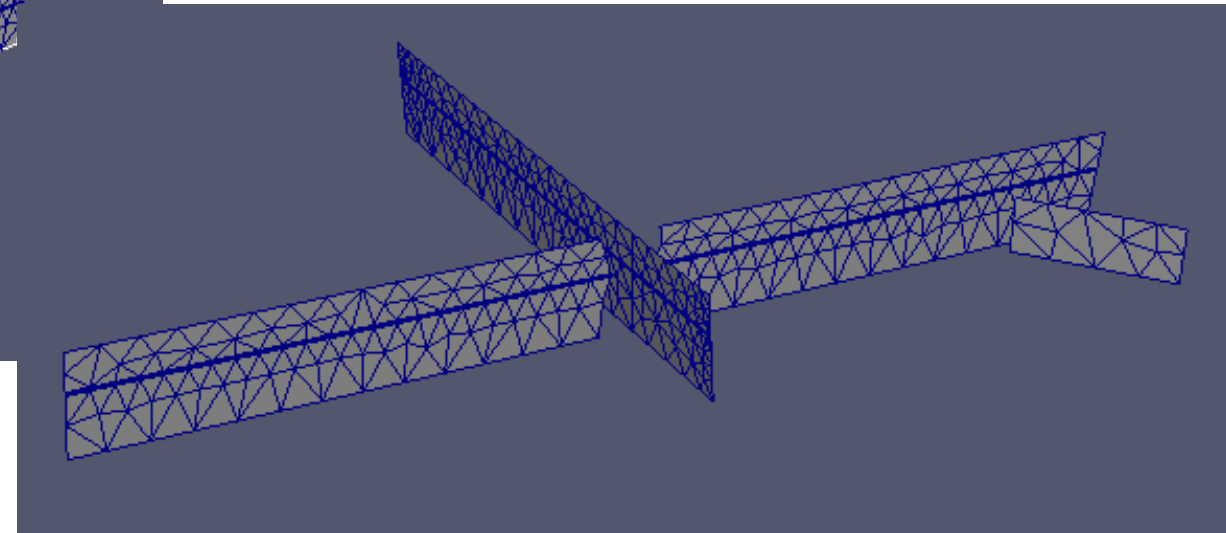
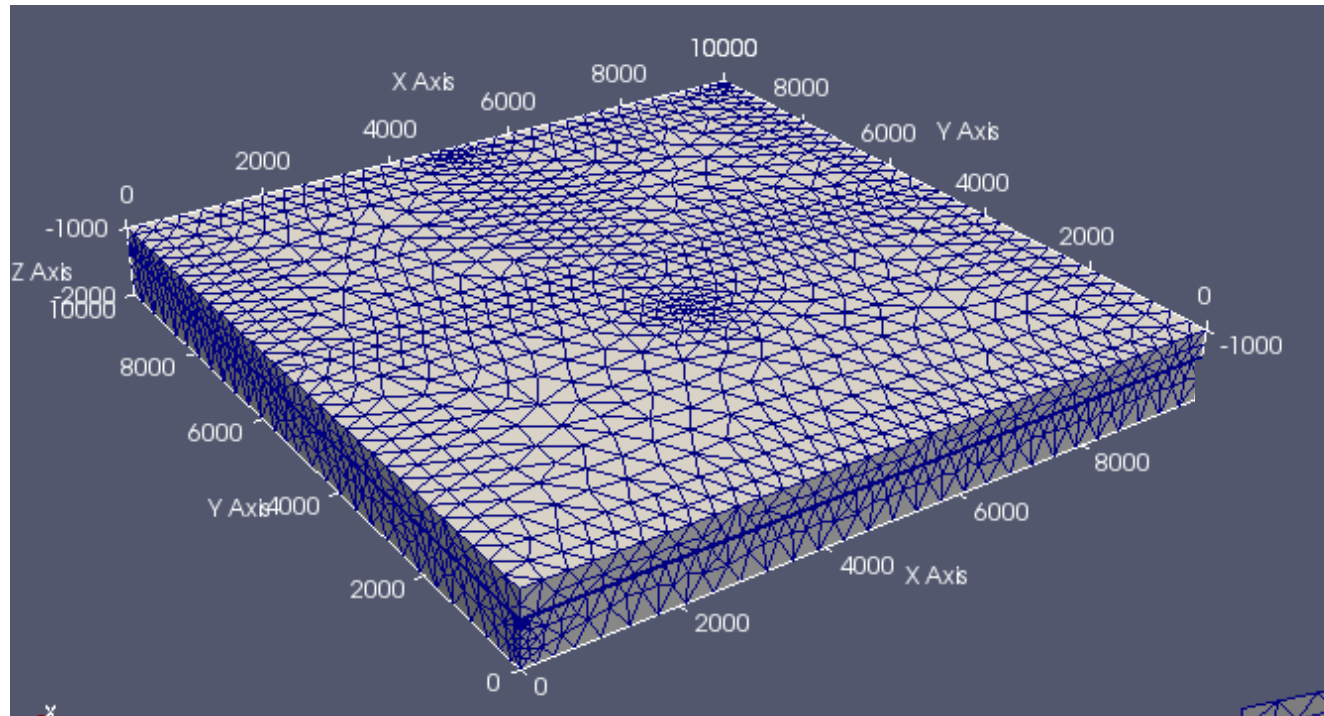
Model domain

- $L_x \times L_y \times L_z = 10 \text{ km} \times 10 \text{ km} \times 1 \text{ km}$
- Three horizons: Morrow Shale Top, Morrow-B Sandstone Top, Morrow-B Sandstone Base
- Three Faults: Fault-1, Fault-3, Fault-6
- Include overburden and underburden



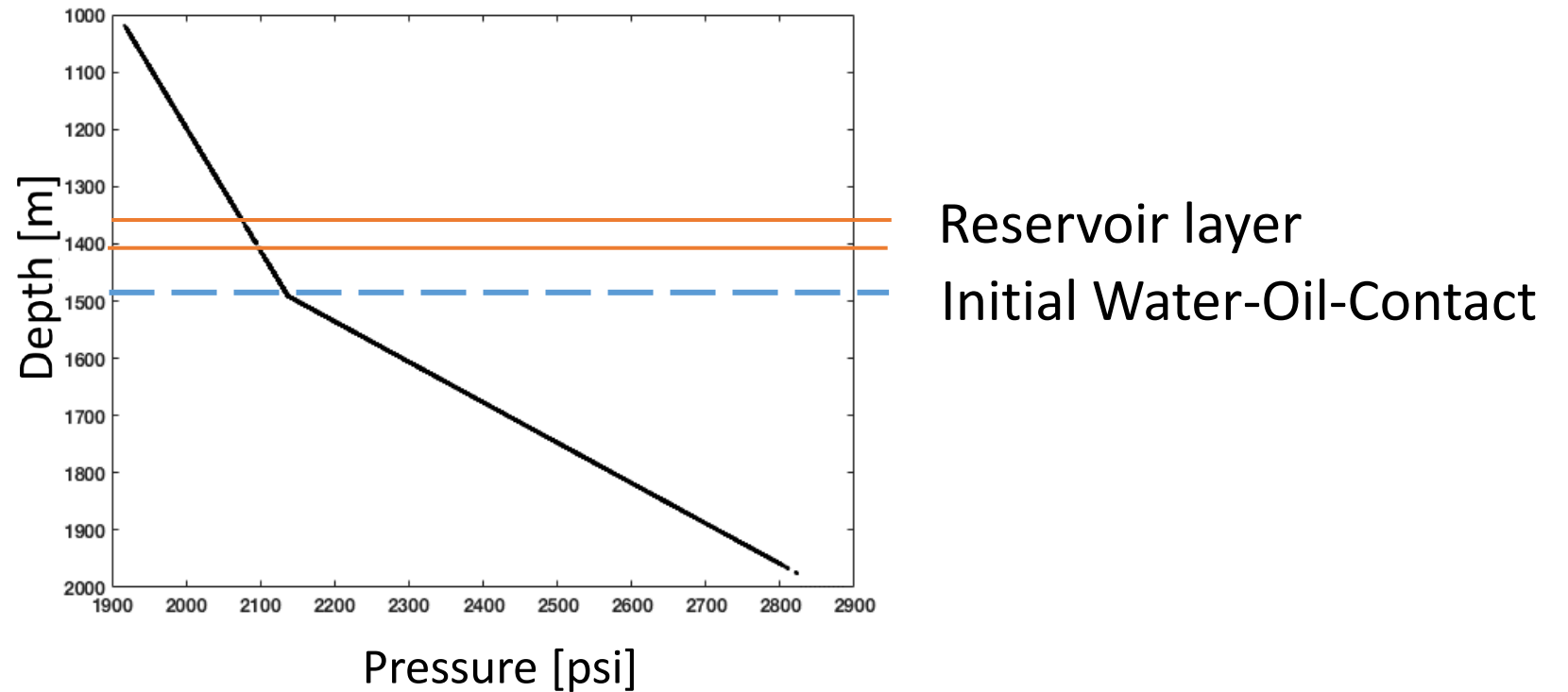
3D Mesh

- Finer mesh within the reservoir and around faults, coarser near the boundaries
- Number of elements = 33,760



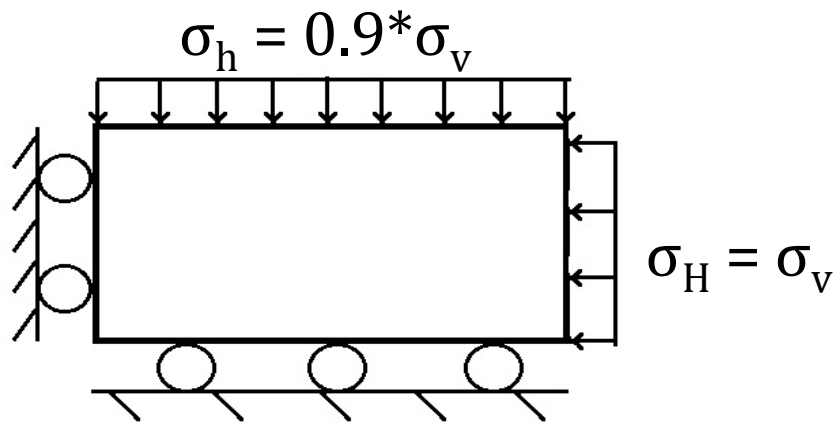
Initial and boundary conditions for Flow

- Initial pressure assumed to be hydrostatic
- Initial water saturation = 0.31
- No-flow boundaries

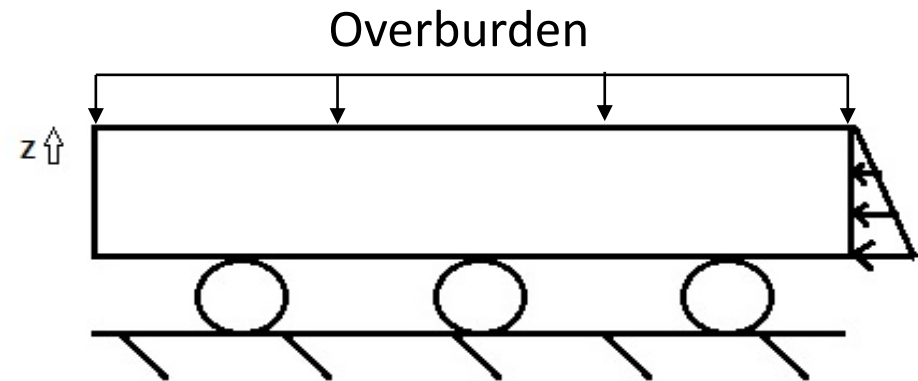


Initial and boundary conditions for Mechanics

- Initial total vertical stress assumed to be lithostatic
- Initial total horizontal stresses from normal faulting stress regime
- Tectonic compression on two sides, overburden on the top boundary, other three boundaries fixed in the normal direction



Top view

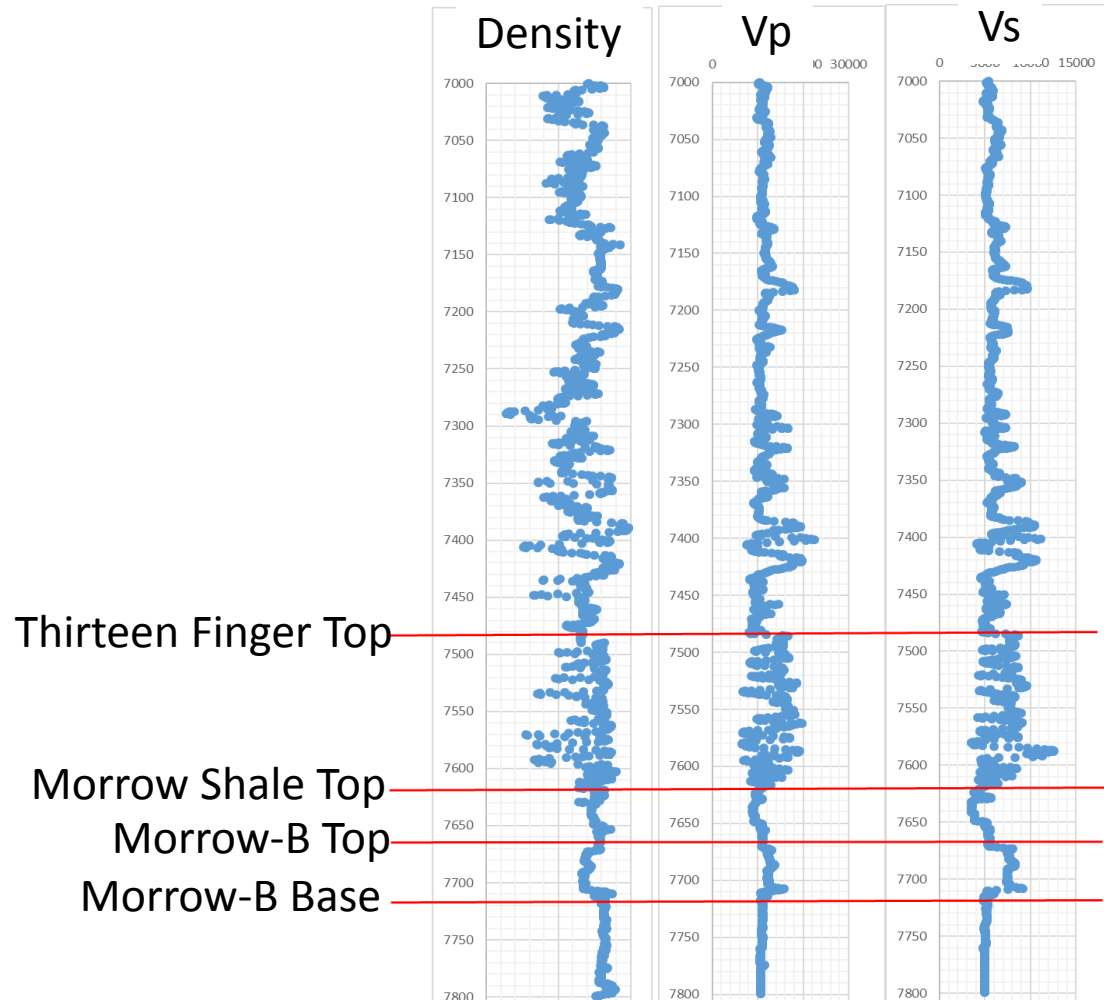


Side view

Distribution of mechanical properties

Bulk density, Young's modulus, Poisson's ratio, Shear modulus obtained from three well logs (Well 13-10A, 13-14, 32-08)

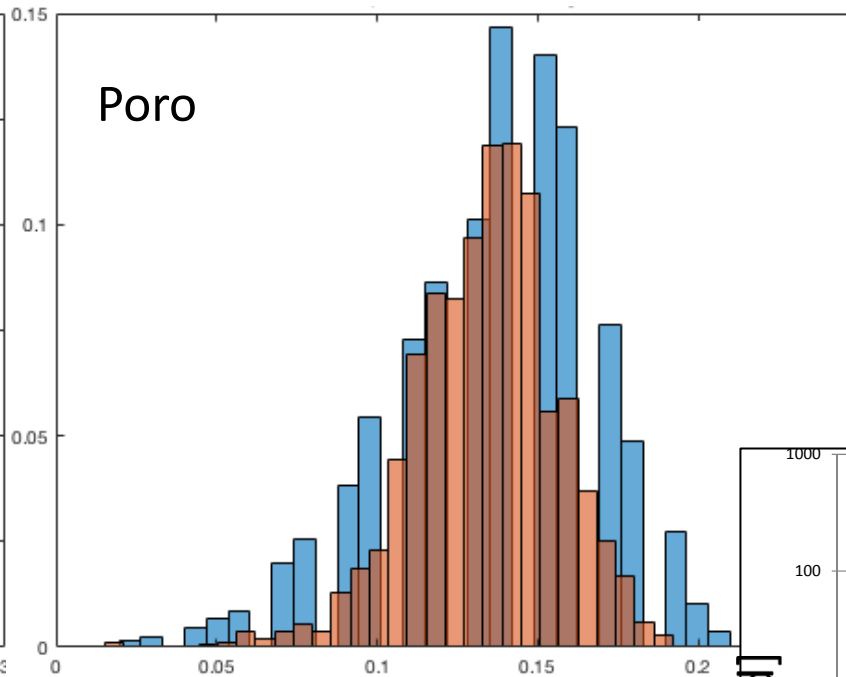
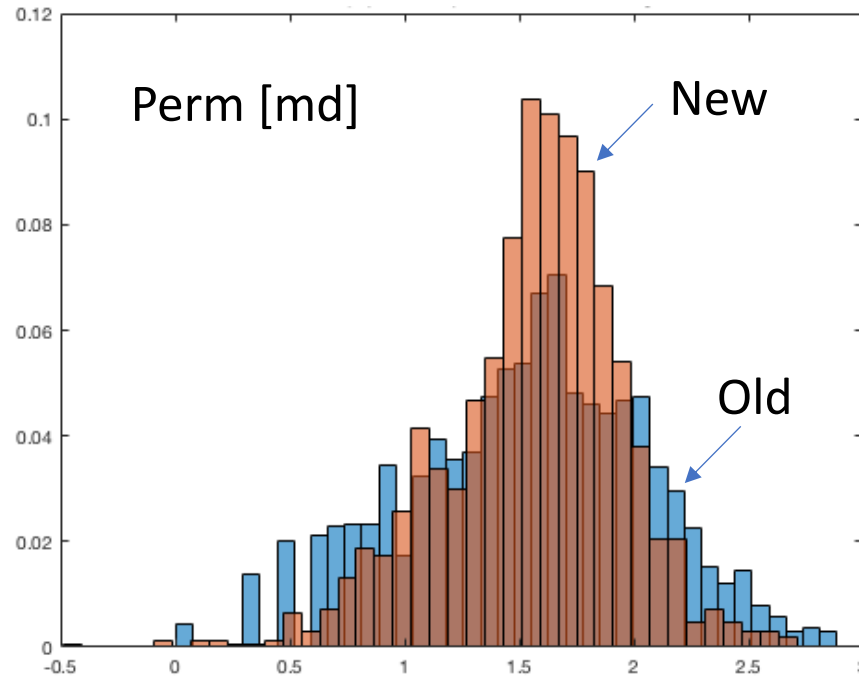
Well 13-10 A



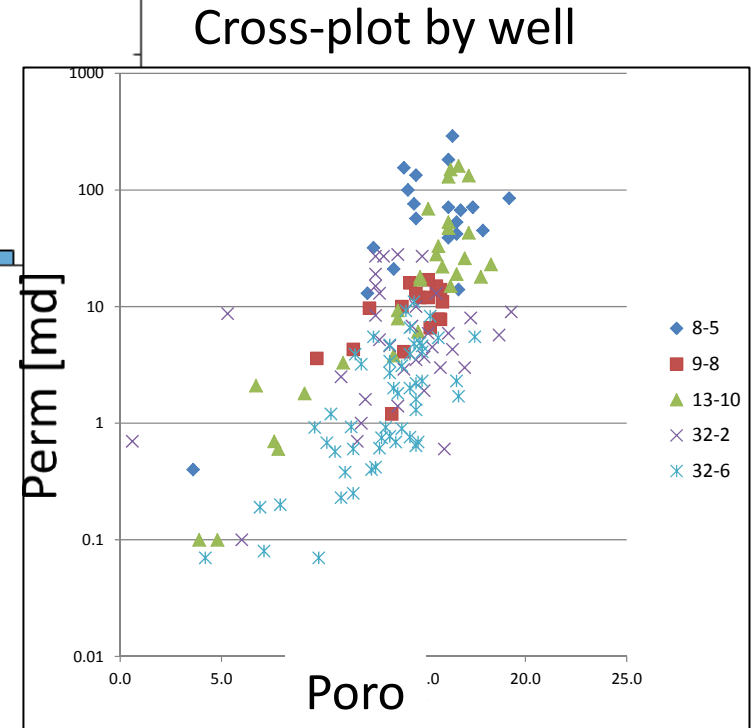
	Avg. density	Avg. Vp	Avg. Vs	K	E
	kg/m ³	m/s	m/s	MPa	MPa
Thirteen Finger Limestone	2518.09	3864.759	2020.616	23,903	26,975
Morrow Shale	2514.793	3121.062	1418.284	17,751	13,859
Morrow B	2402.182	3834.89	2317.973	18,118	31,290
average	2480	3600	1920	19,951	23,792

Distribution of flow properties

Map porosity and permeability from an old Eclipse model



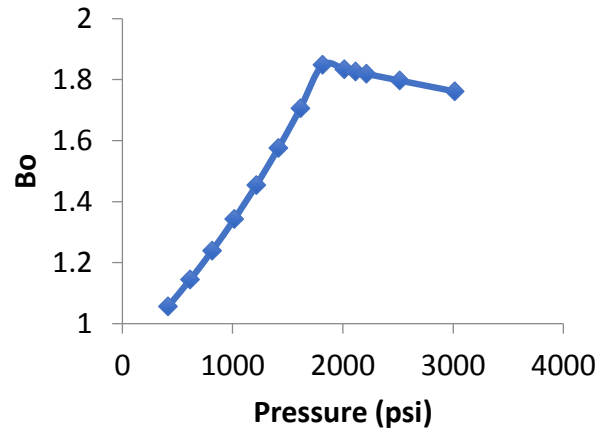
These show that the mapping process is able to preserve the mean and std dev of the property.



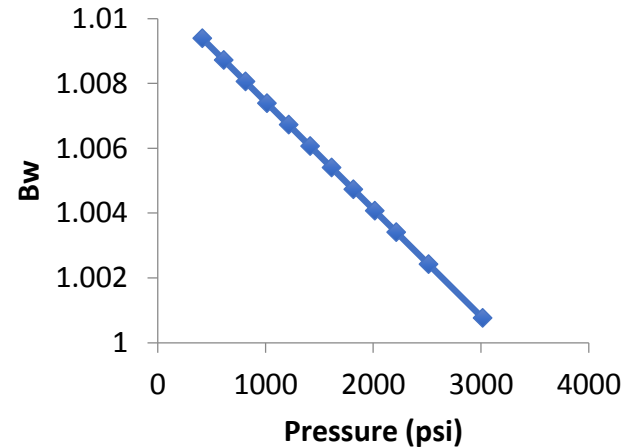
Multiphase flow properties

- Convert the old compositional model into a Black-Oil model using differential liberation simulation

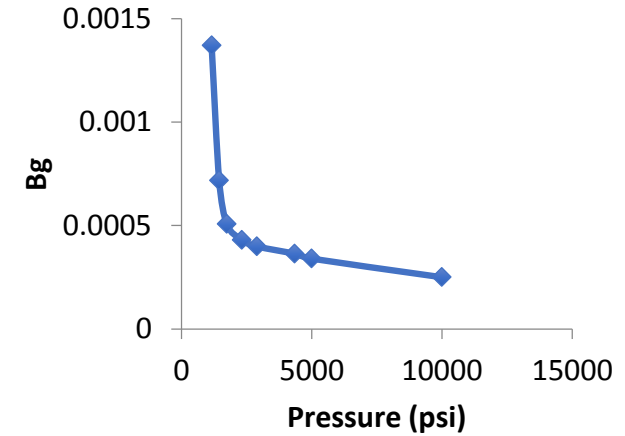
Oil compressibility



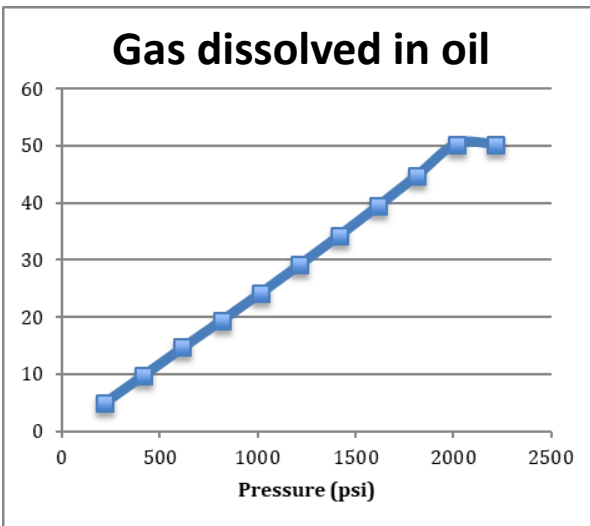
Water compressibility



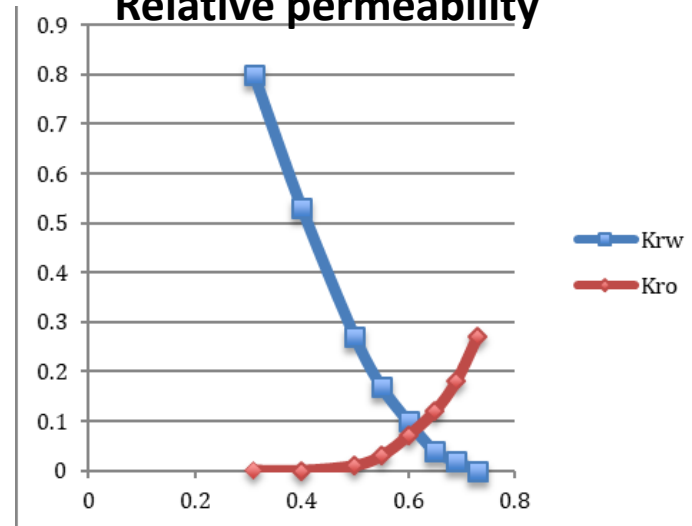
Gas compressibility



Gas dissolved in oil

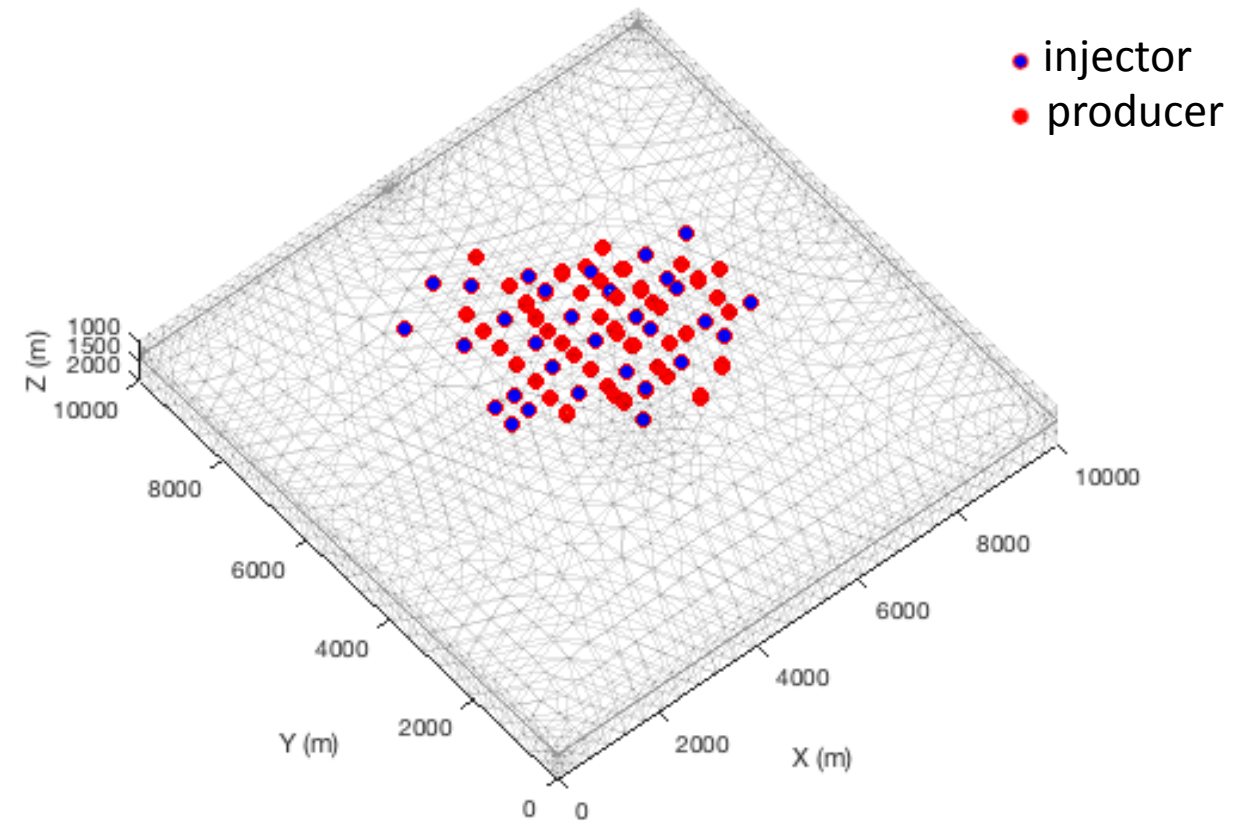
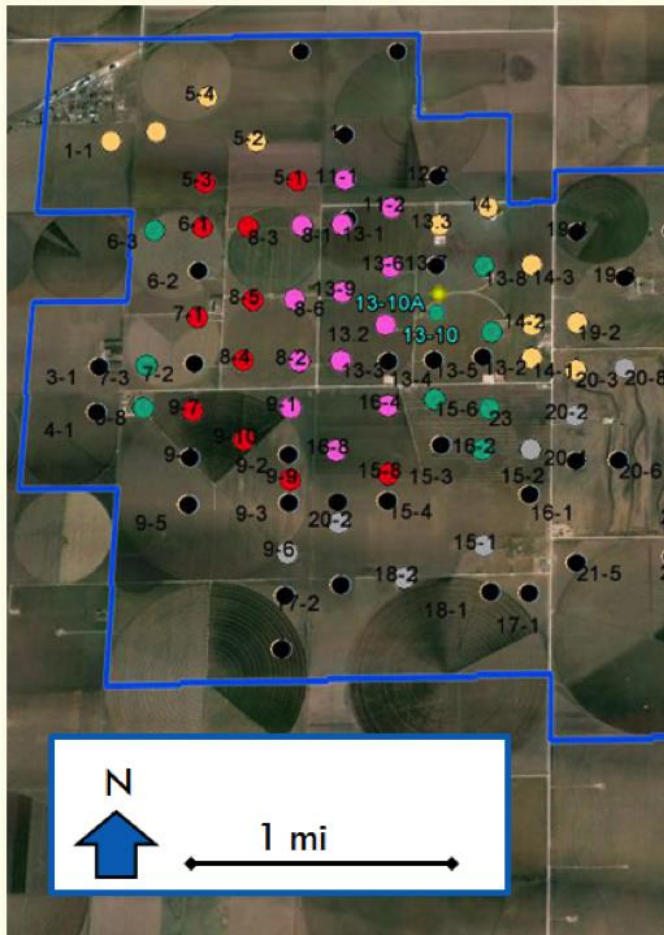


Relative permeability



Well model

- Total 76 wells, 45 producers, 31 injectors (water and CO2 injectors)
- Project all wells into the geomechanical model by intersecting the trajectories with the 3D mesh

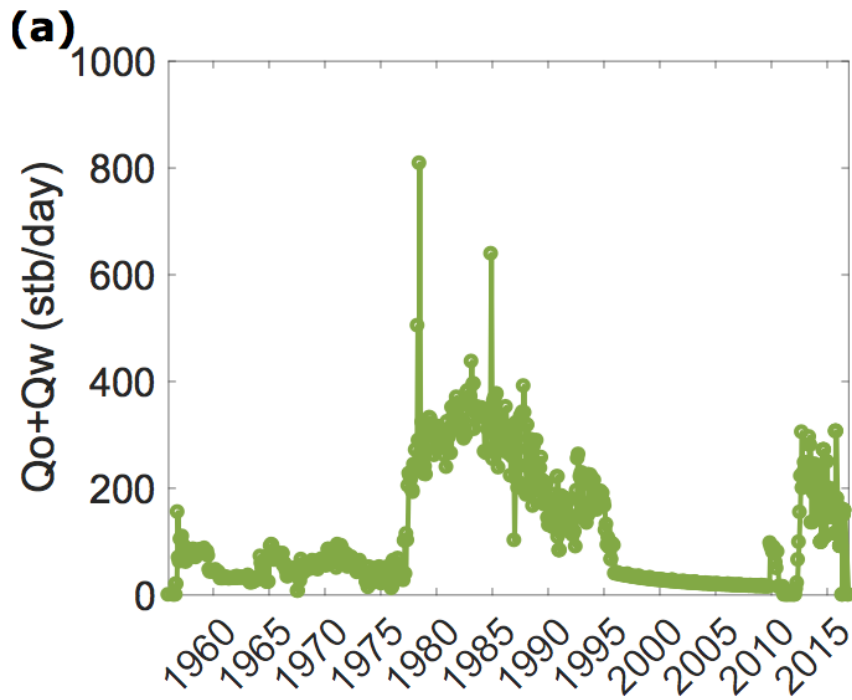


Coupled Simulation

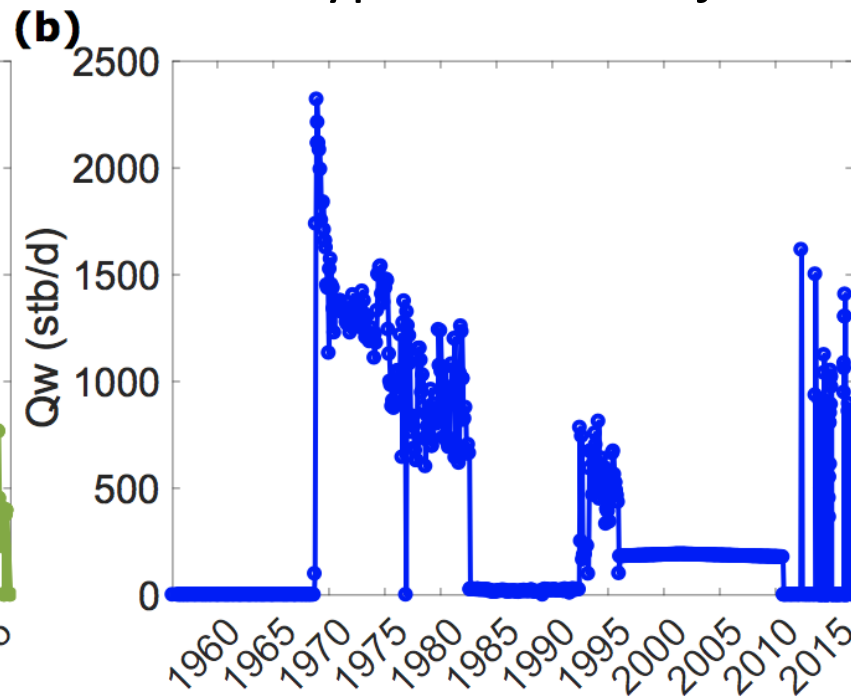
- Simulation period: January 1956 to July 2016
- Impose liquid (oil + water) production schedule (volume vs. time) at producers and injection schedule at injectors
- Results
 - Well rate and well bottomhole pressure
 - Change in the reservoir average pressure
 - Vertical and horizontal displacement in the reservoir and caprock
 - Change in the fault pressure
 - Coulomb stress change on the faults

Historical well rates used to drive/calibrate the simulation

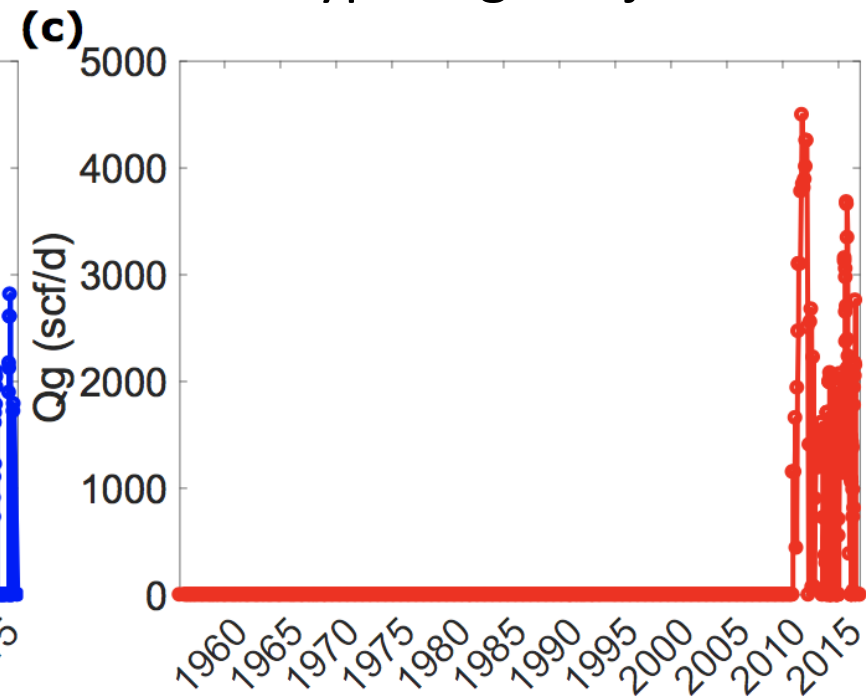
Typical producer



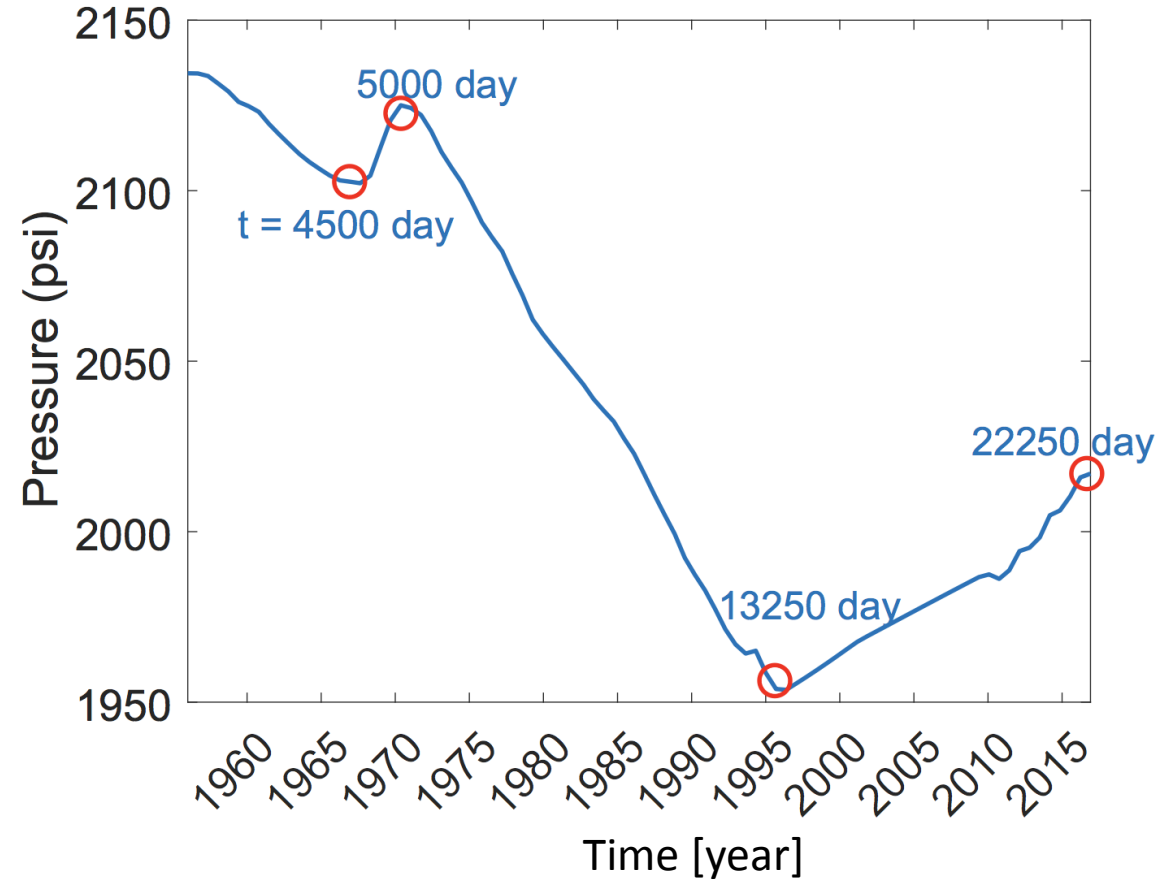
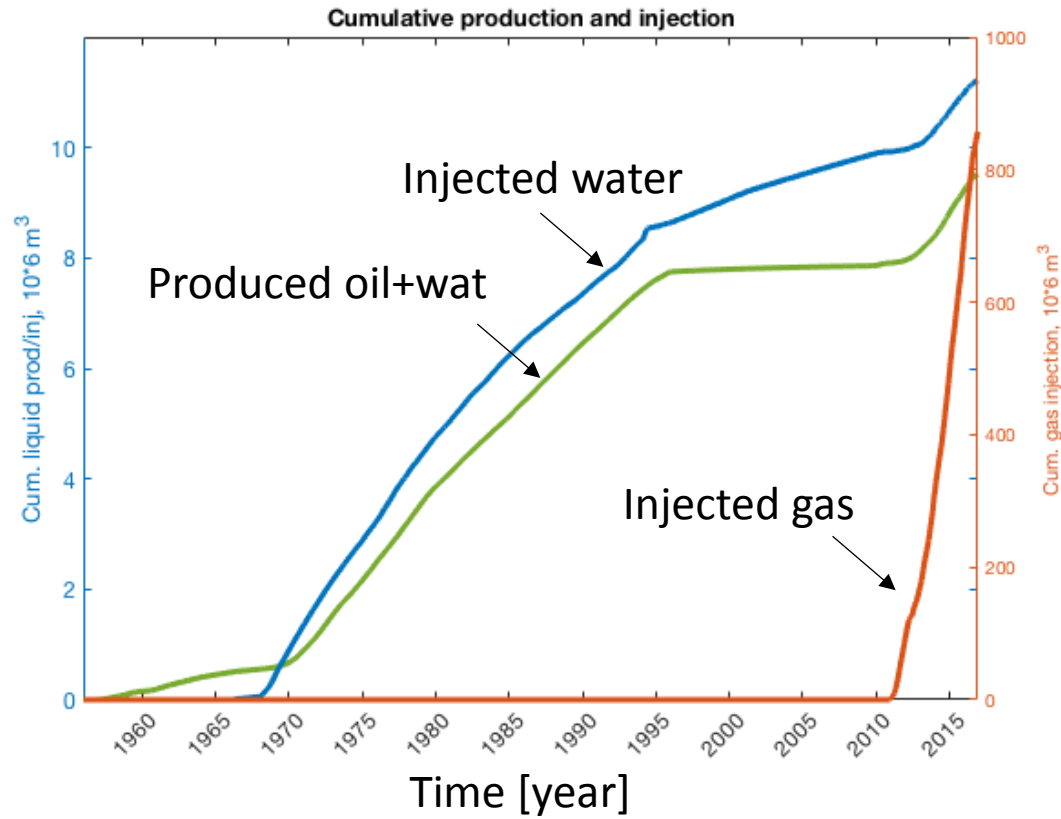
Typical water injector



Typical gas injector

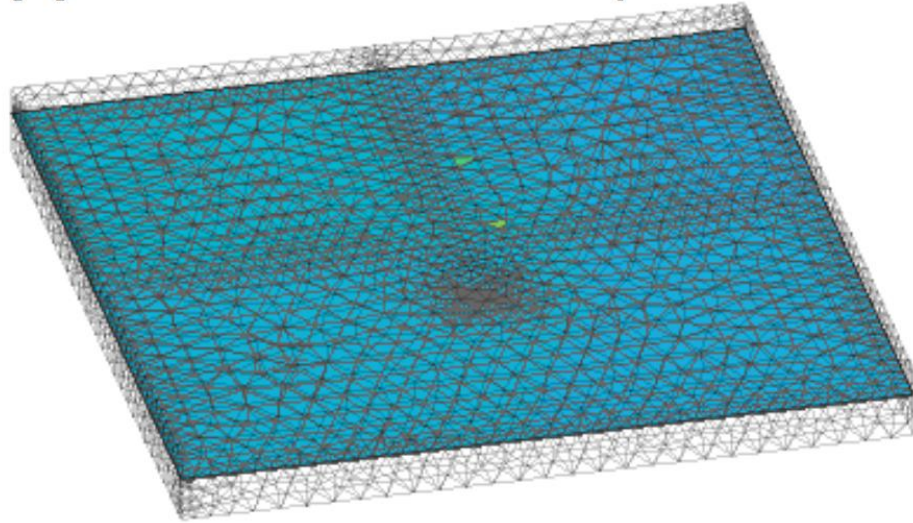


Cumulative production and average pressure evolution

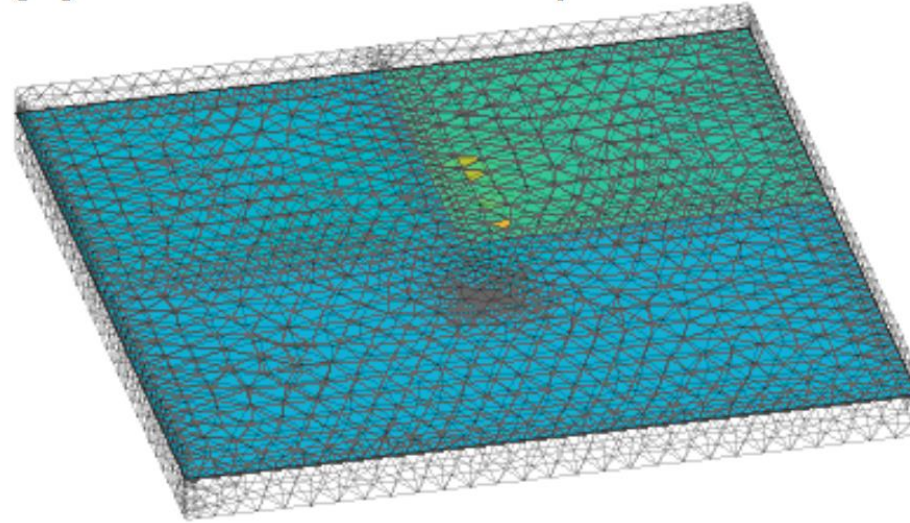


Change in the reservoir pressure

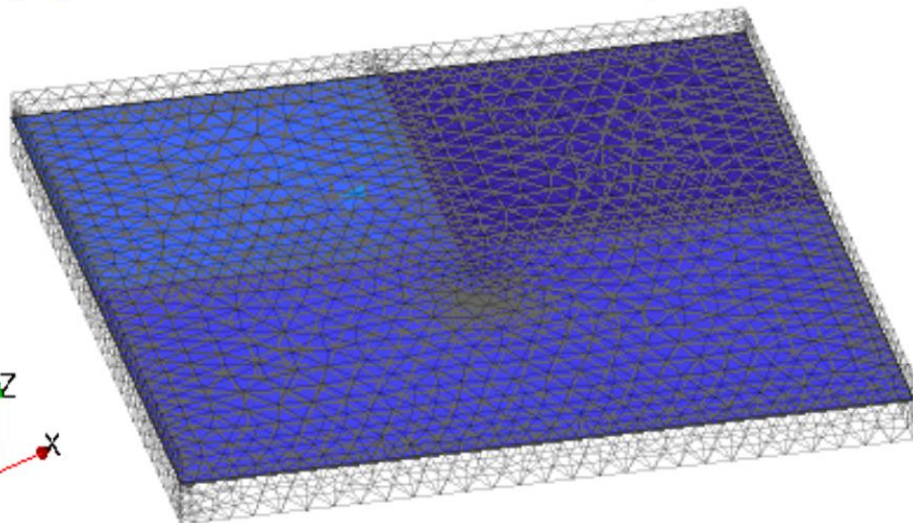
(a) $t = 4500$ day



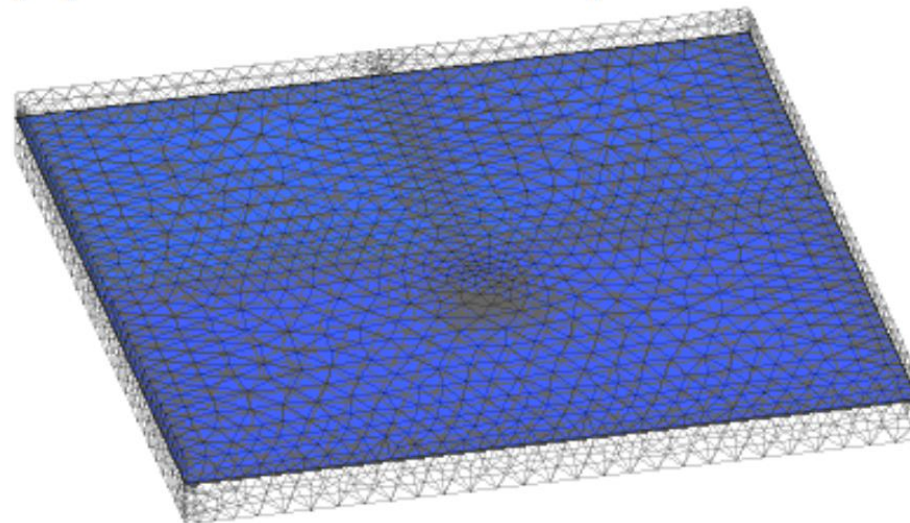
(b) $t = 5000$ day



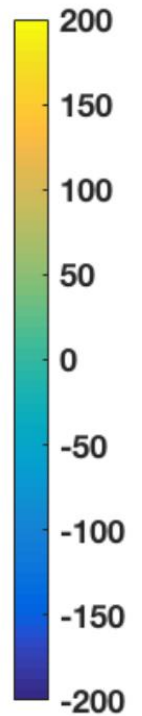
(c) $t = 13250$ day



(d) $t = 22250$ day

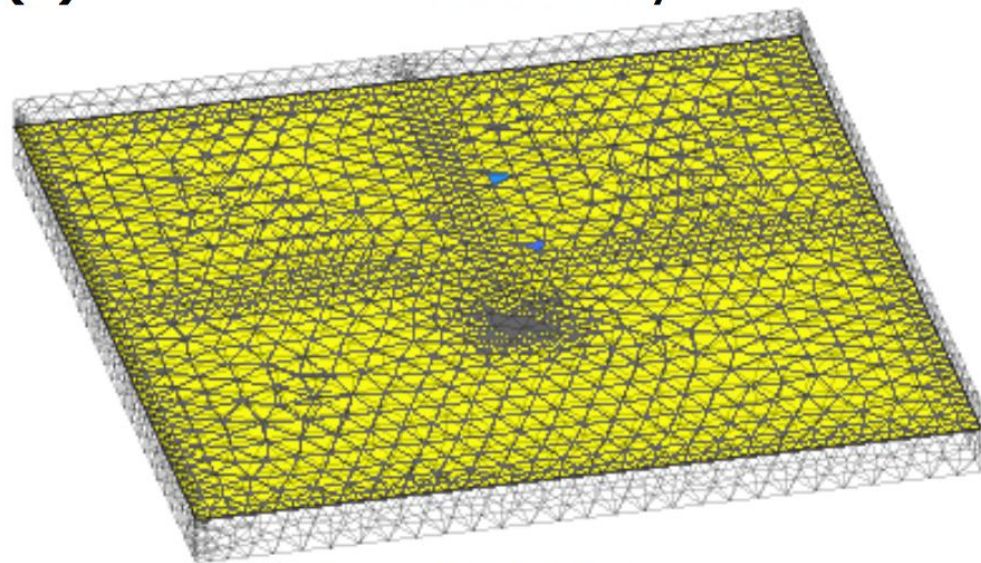


Pressure [psi]

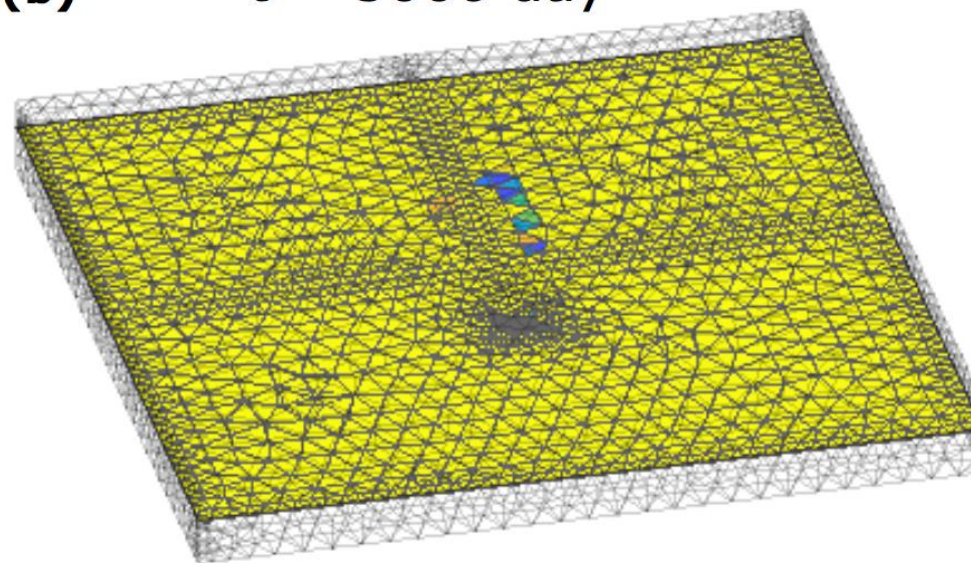


Change in the reservoir oil saturation

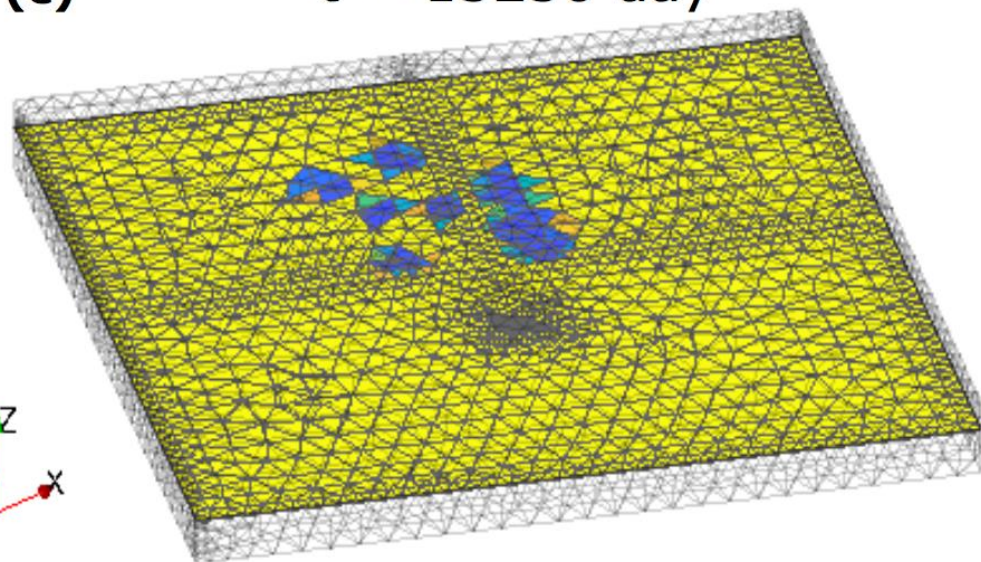
(a) $t = 4500$ day



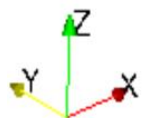
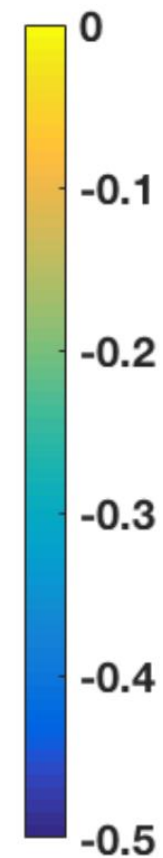
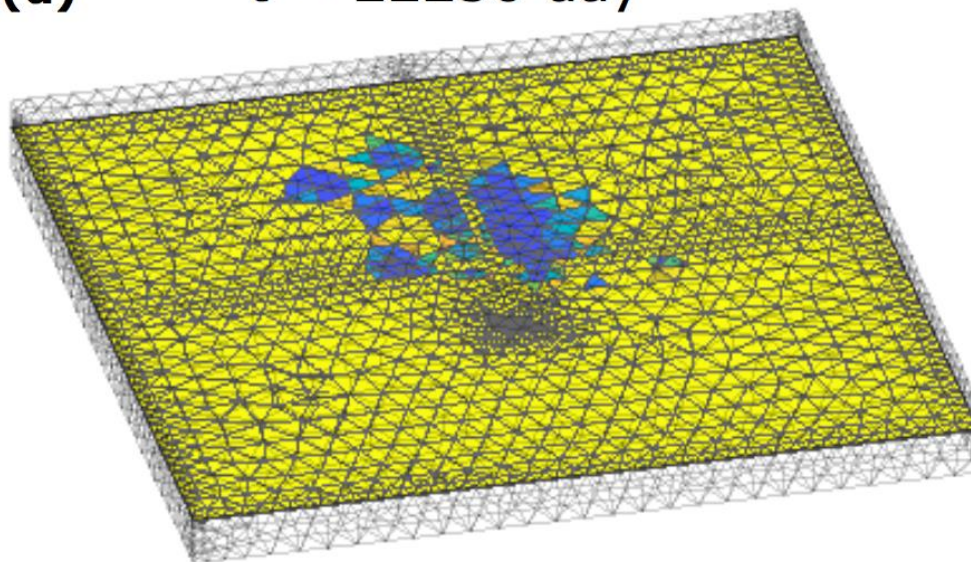
(b) $t = 5000$ day



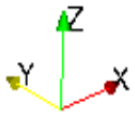
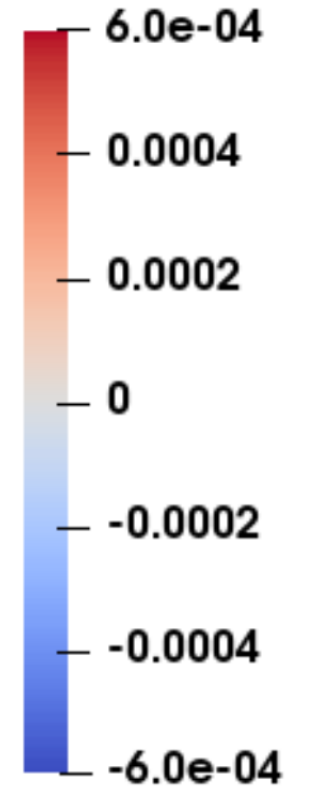
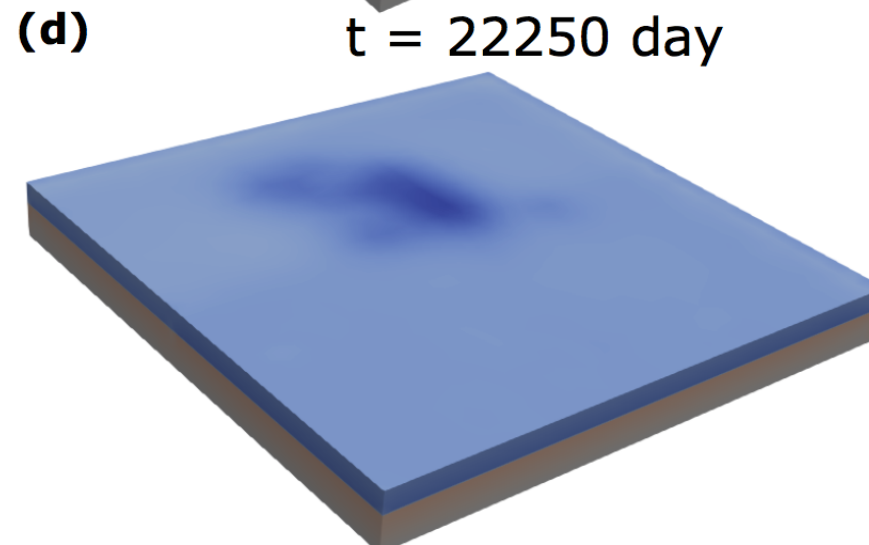
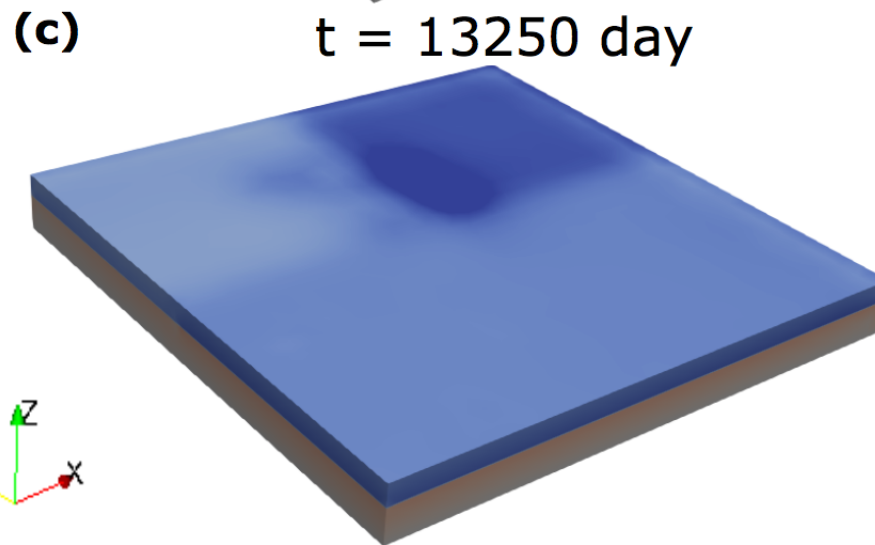
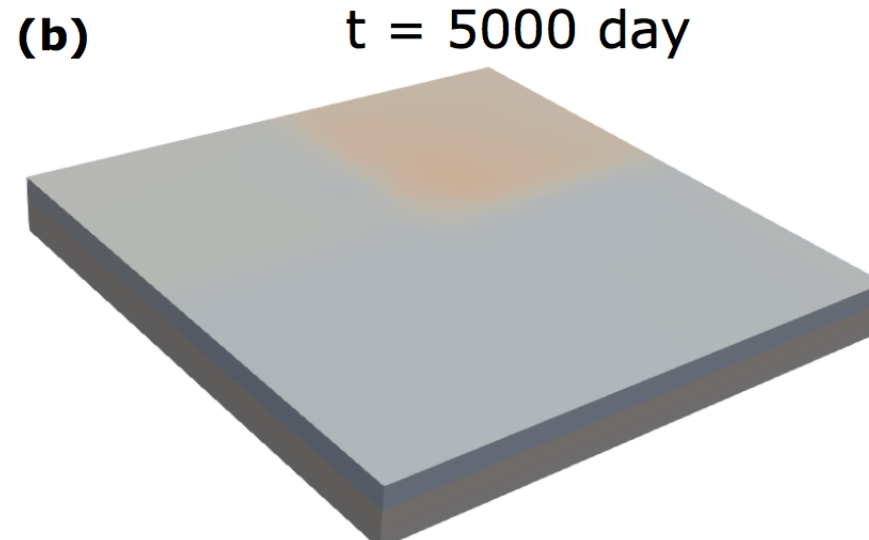
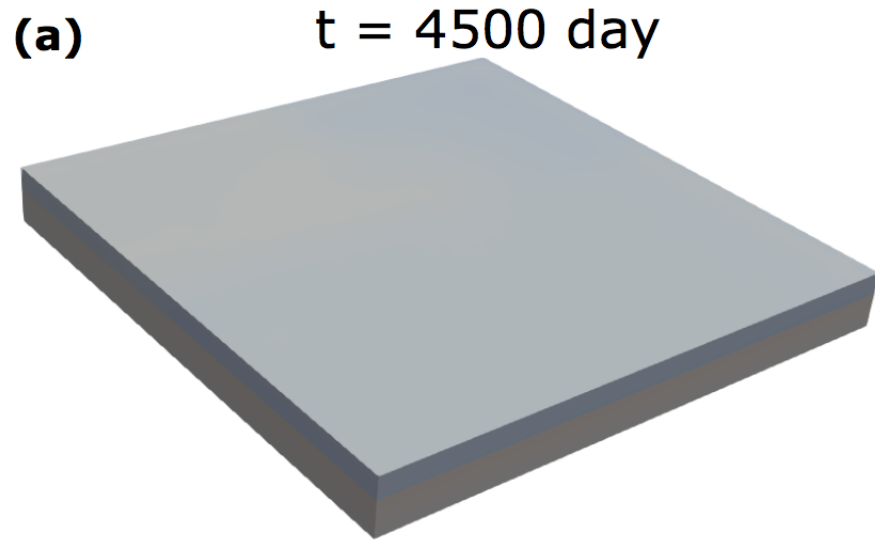
(c) $t = 13250$ day



(d) $t = 22250$ day

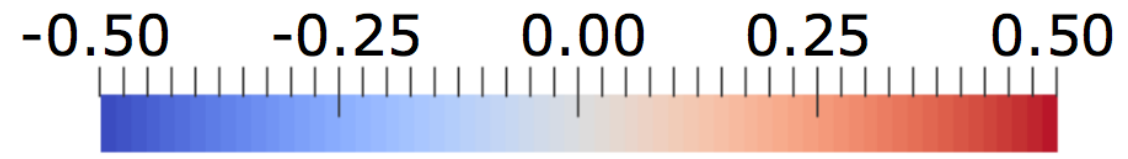
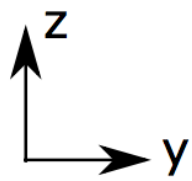
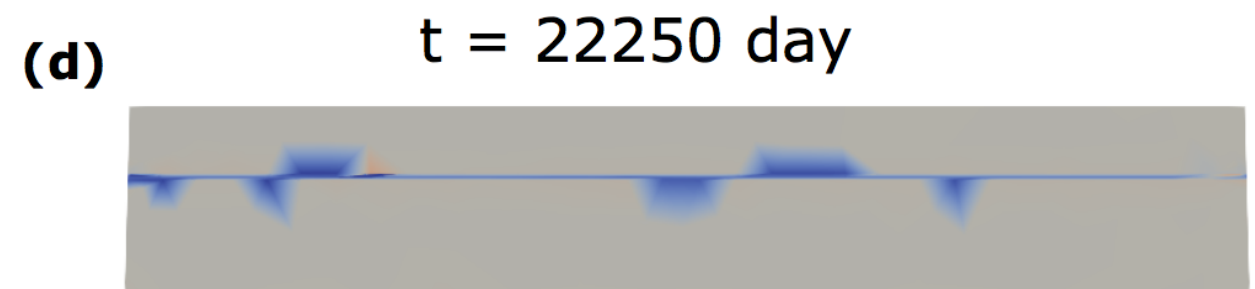
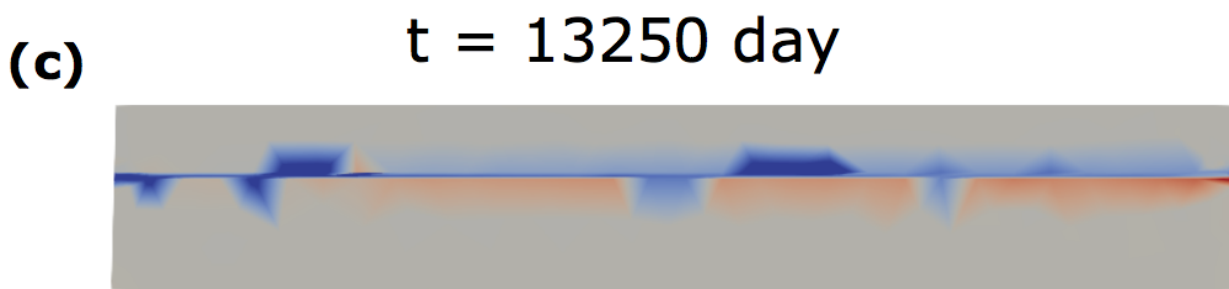
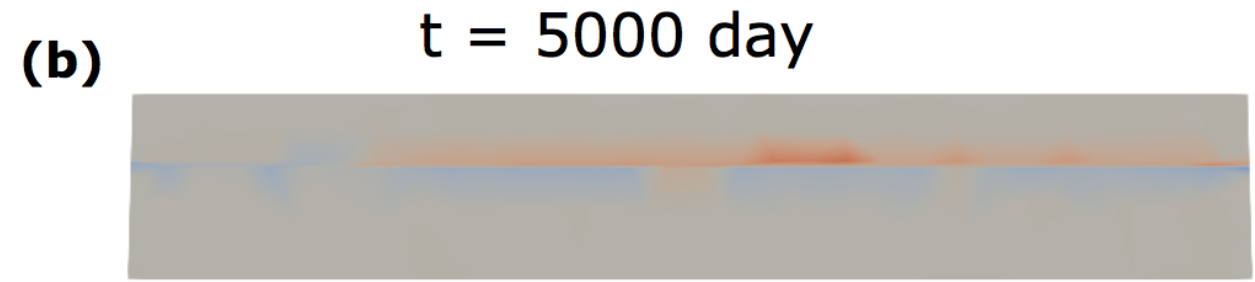
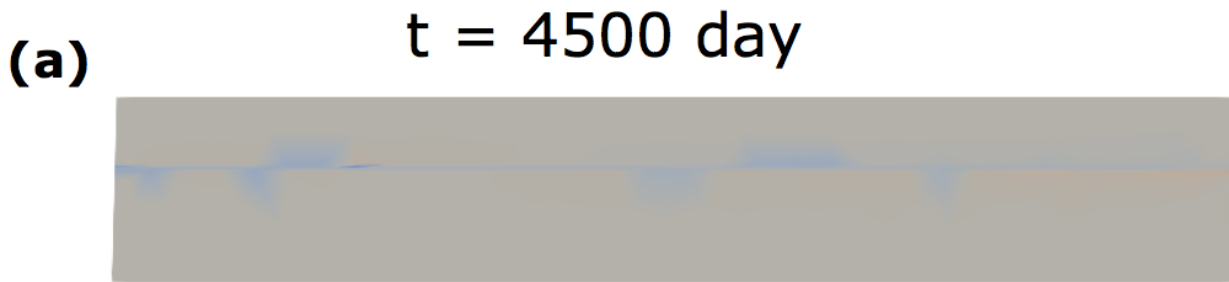


Vertical displacement

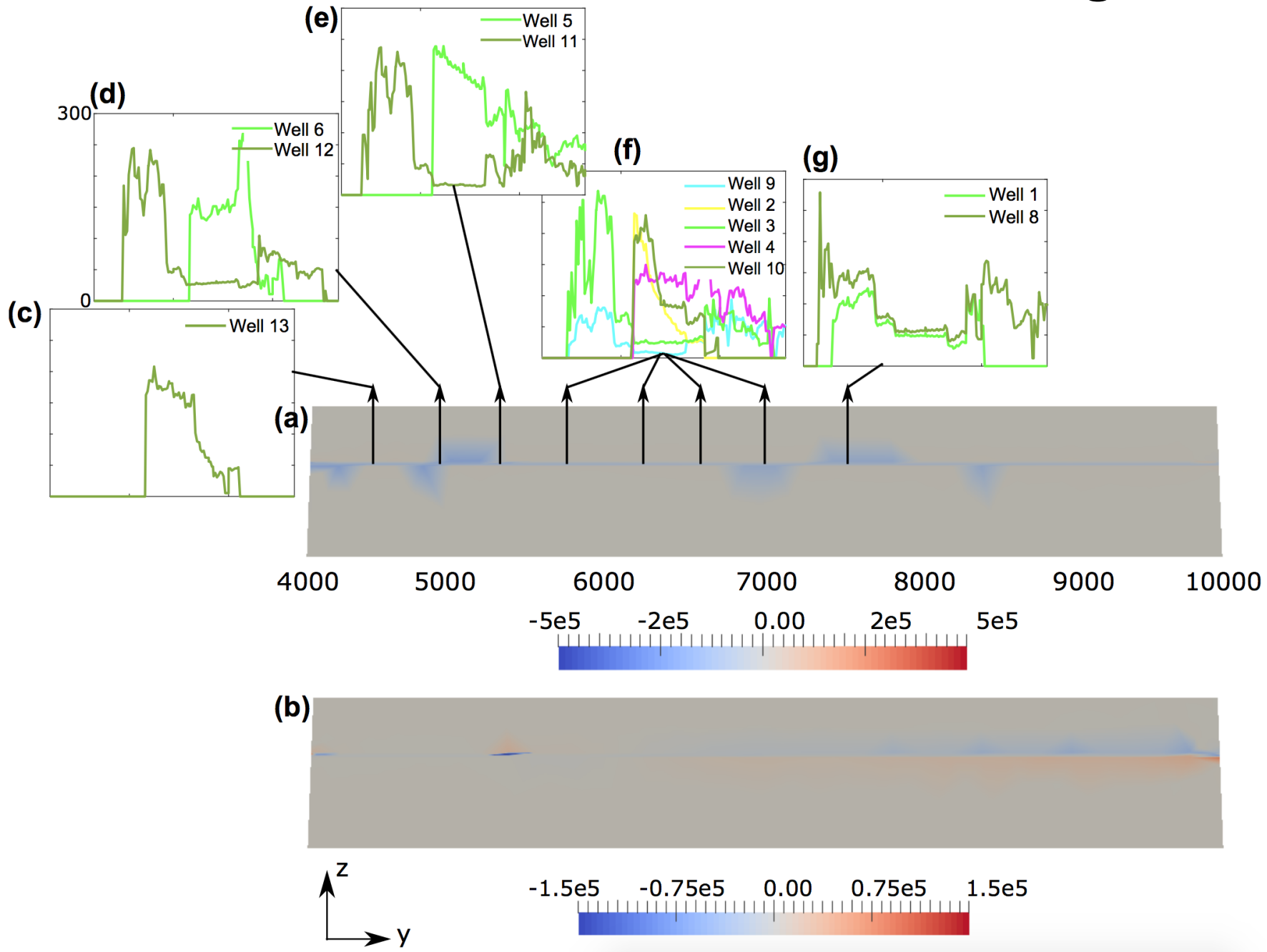


Change in the Coulomb stress on a fault

$$\Delta\text{CFF} = \Delta\tau + \mu_f \Delta\sigma'_n$$



Well activities can be correlated to stress changes on a fault



Geomechanical Experiments

Objective: Perform geomechanical testing at nano, micro, and macro scales. Understand the effect of scale and lithology on the CO₂-induced changes in properties.

Farnsworth Cores

Sample ID	Diam., mm	Length, mm	Depth, feet	Well #	Porosity %	Permeability, mD
A1	25.52	45.72	7631	13-14	5.0	2.5E-3
A2	25.35	55.70	7553	13-10A	5.8	2.7E-3
A3-1	25.62	59.29	7682	13-14	1.3	4.0E-5
A3-2	25.60	55.64	7682	13-14	2.0	9.4E-4
B2	25.56	56.98	7680	13-10A	12.9	2.3



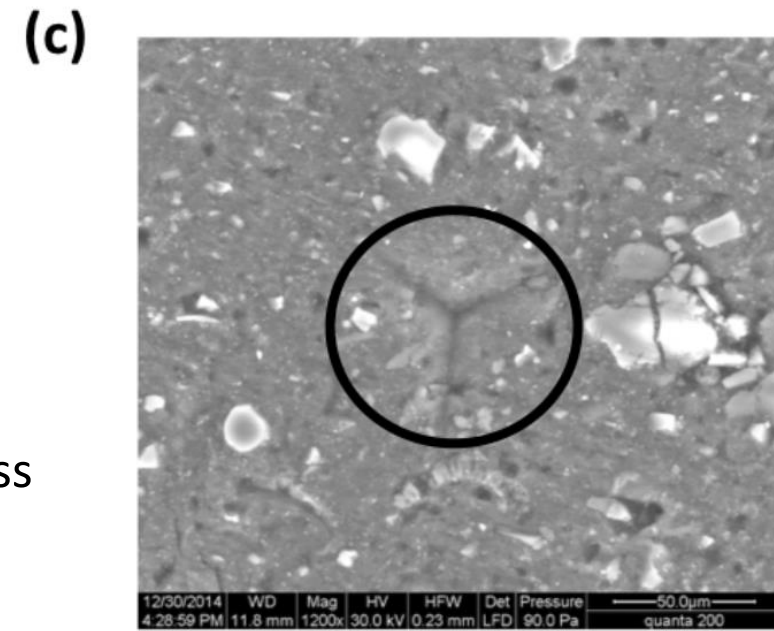
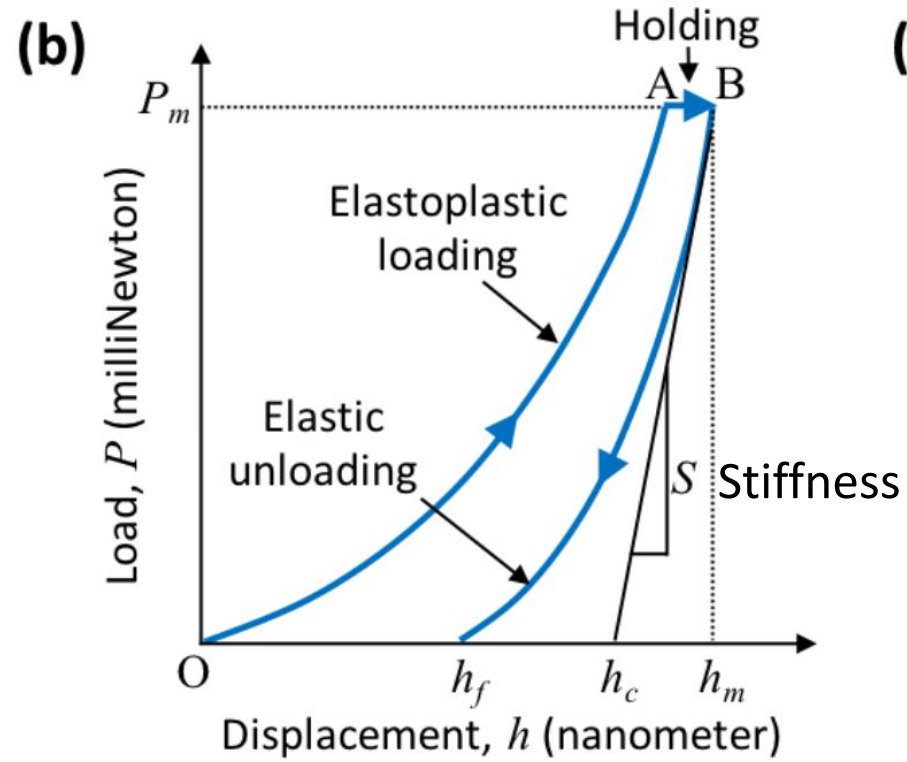
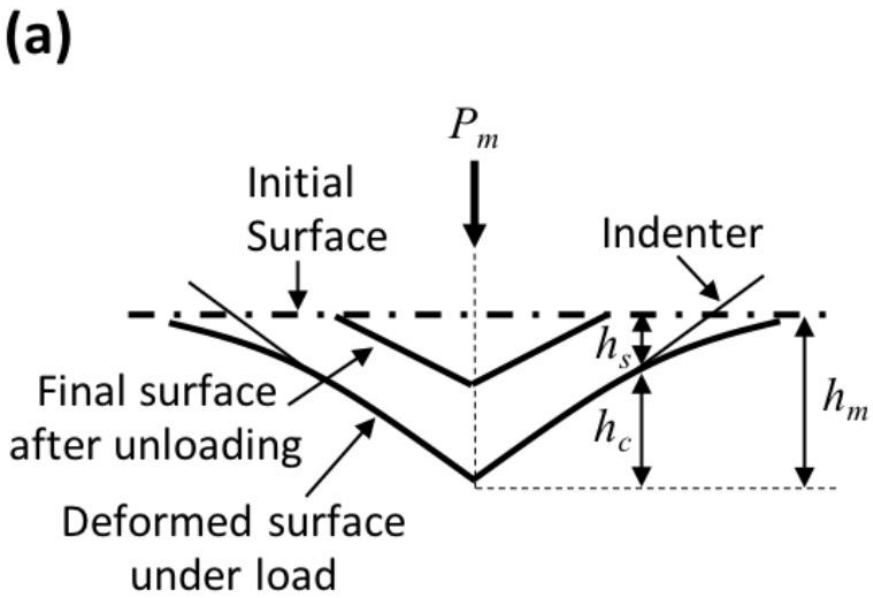
Porosity and permeability measured using a Helium porosimeter HP-401 and a Pulse decay permeameter PDP-200.

Experiments conducted

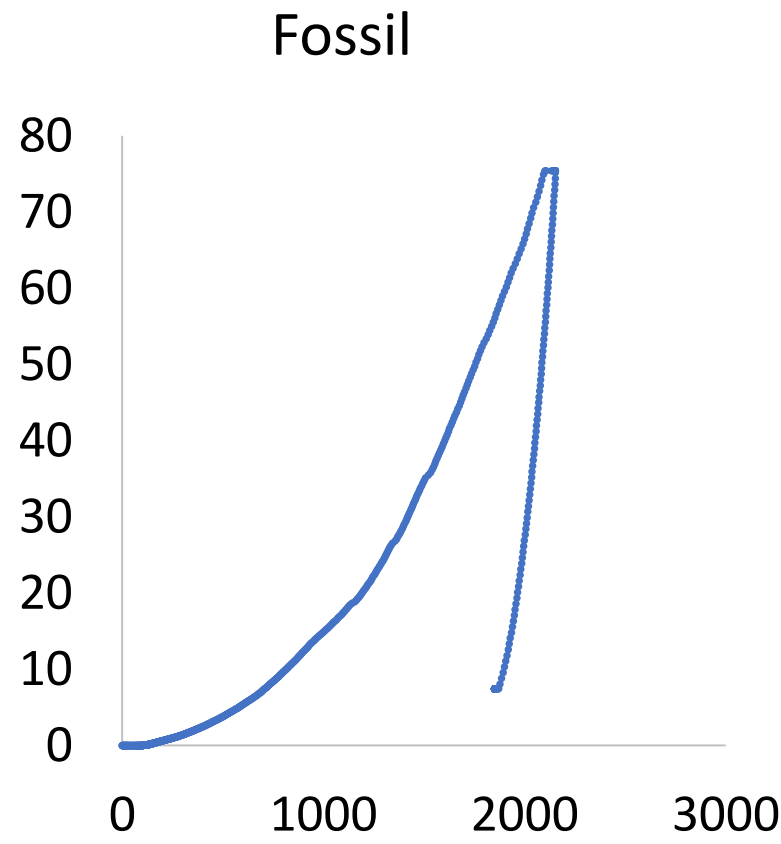
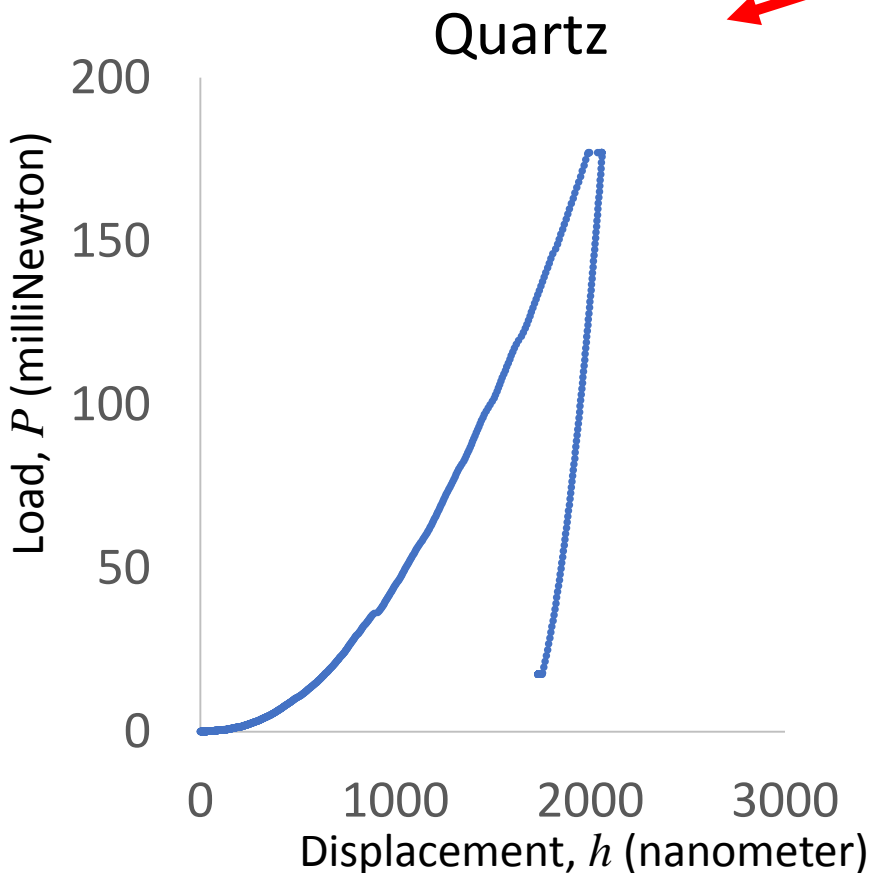
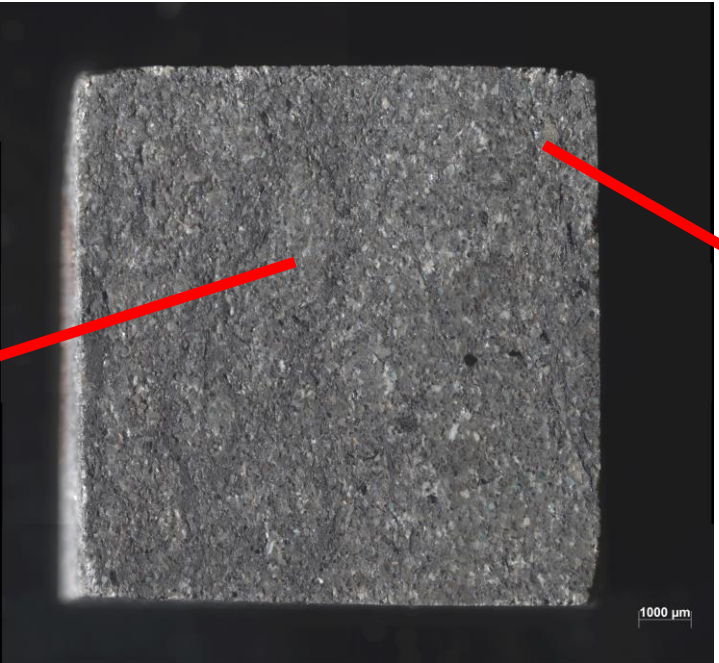
Scale	Experiments	Geomechanical properties
Nano	Nanoindentation	Young's modulus & Fracture toughness before and after CO2 exposure
Micro	Microscratch	Fracture toughness before and after CO2 exposure
Macro	Biaxial load testing	Dynamic Young's modulus & Fracture toughness at different CO2 pressures & temperatures

Spectroscopy and CT scanning are performed for composition and microstructure.

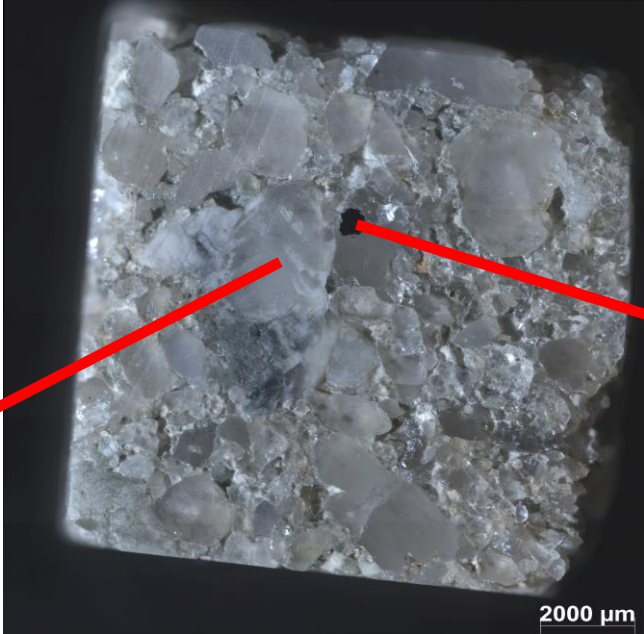
Nanoindentation



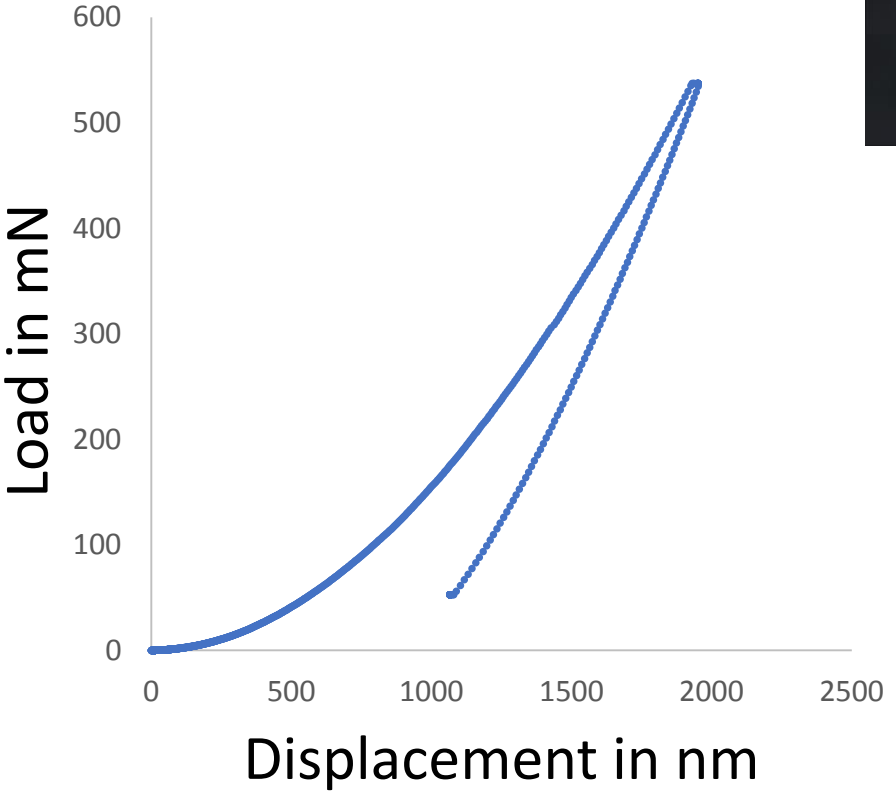
Mudrock indentation



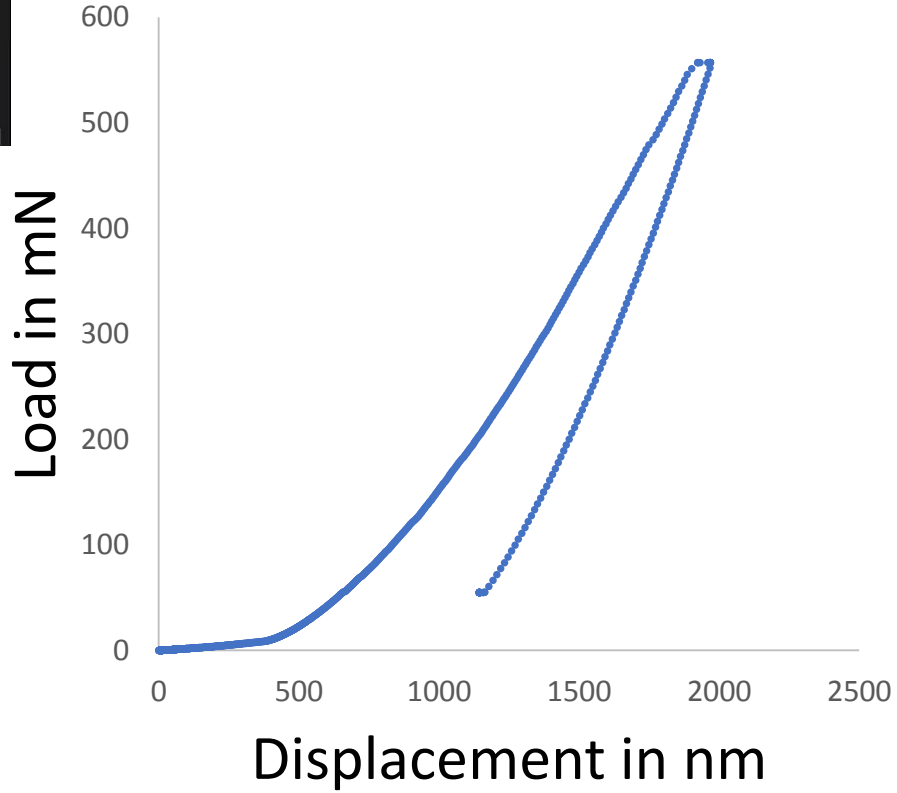
Sandstone indentation



Quartz



Biotite

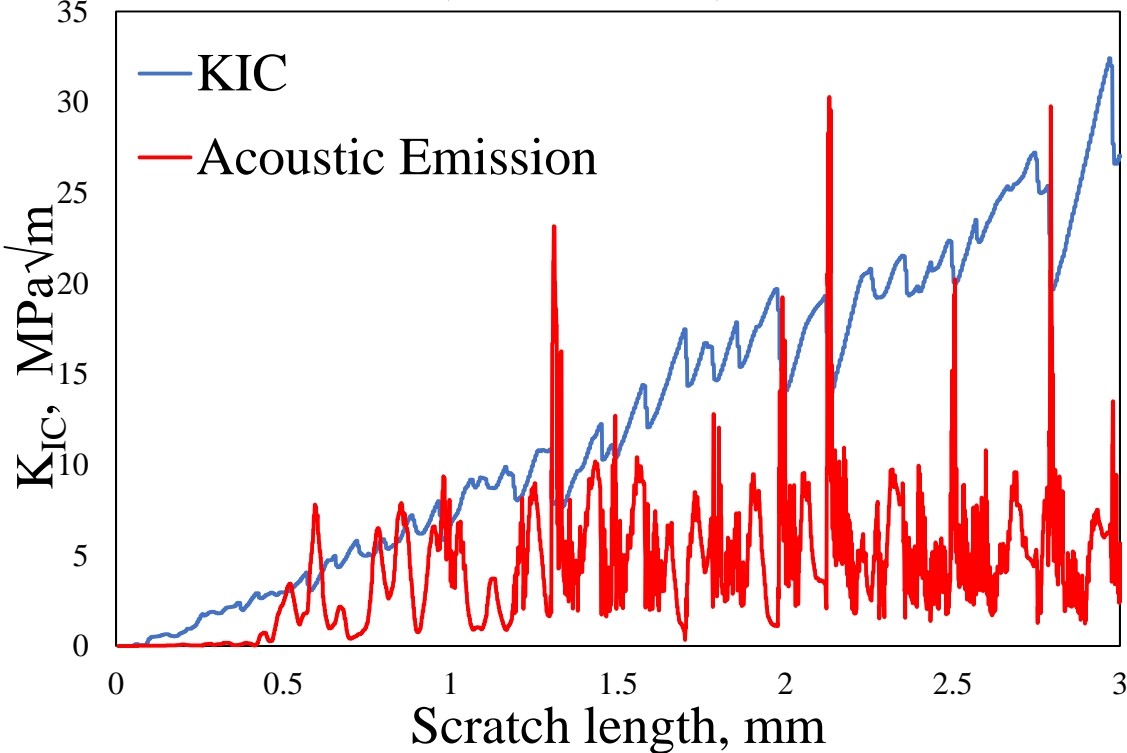


Different stiffnesses and elastic moduli

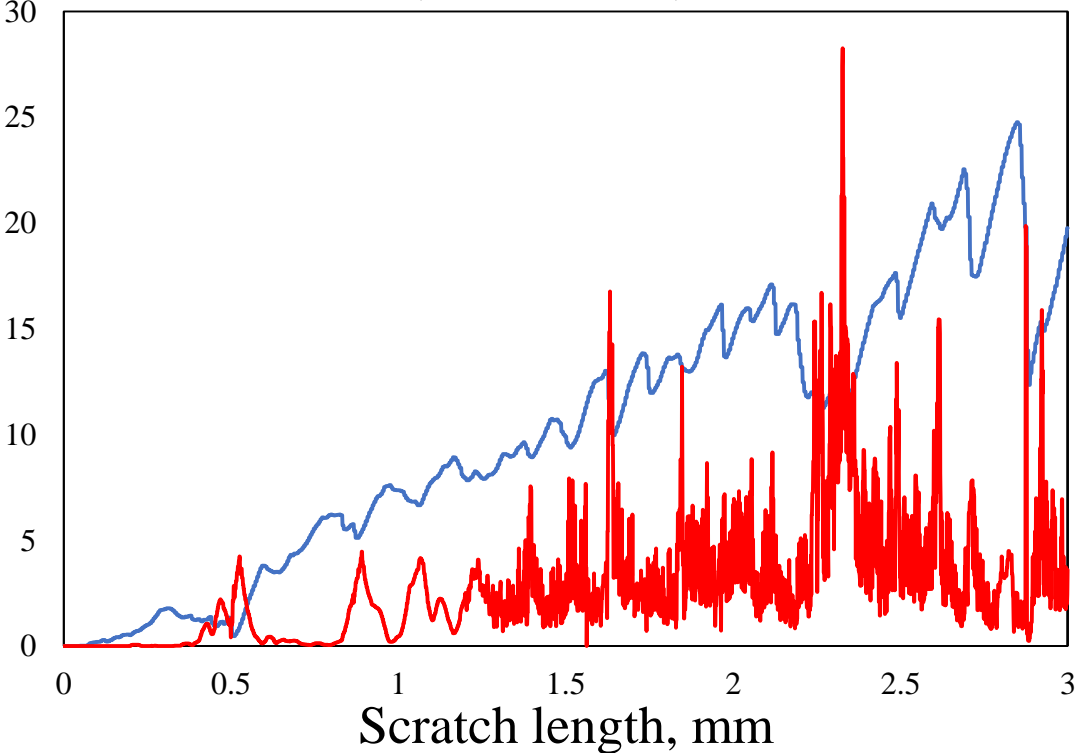
Microscratch

Mudrock

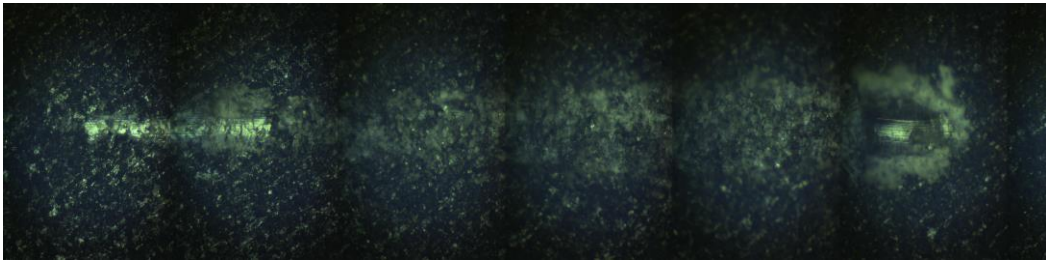
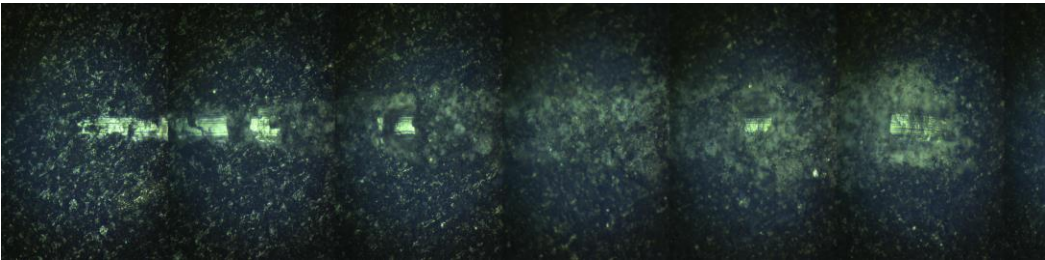
A1 scratch#3, Horizontal, well 13-10A



A3 scratch#3, Horizontal, well 13-14



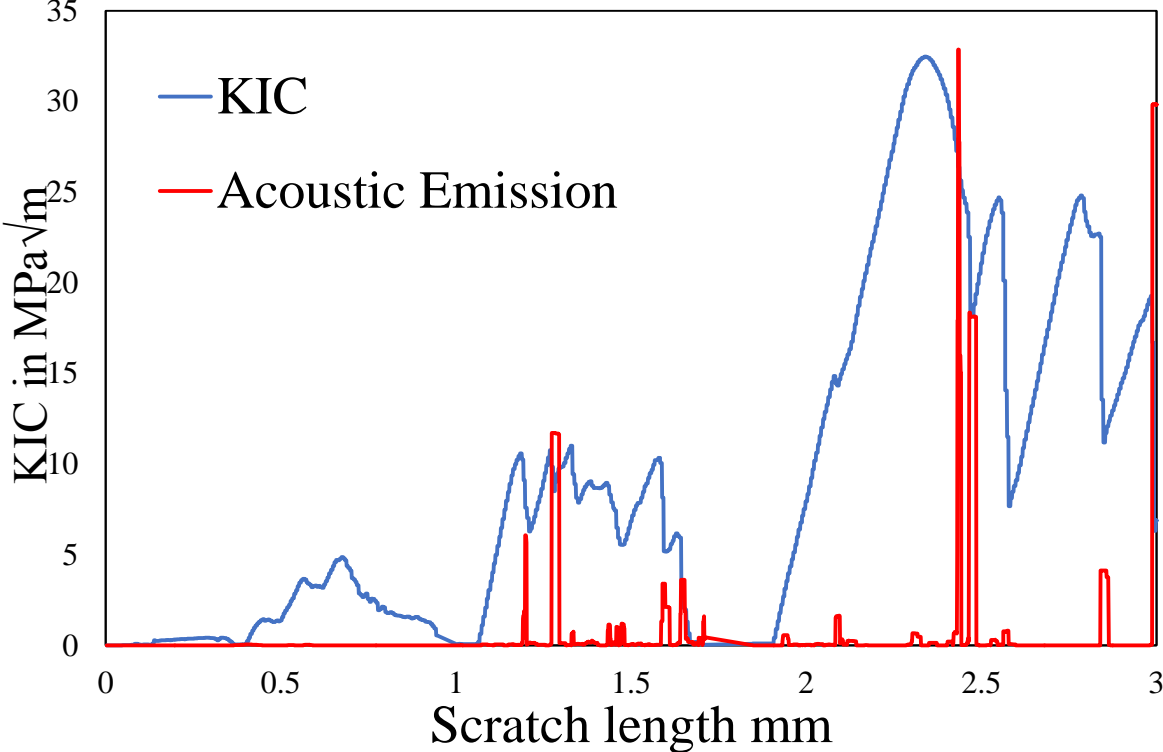
Scratch track



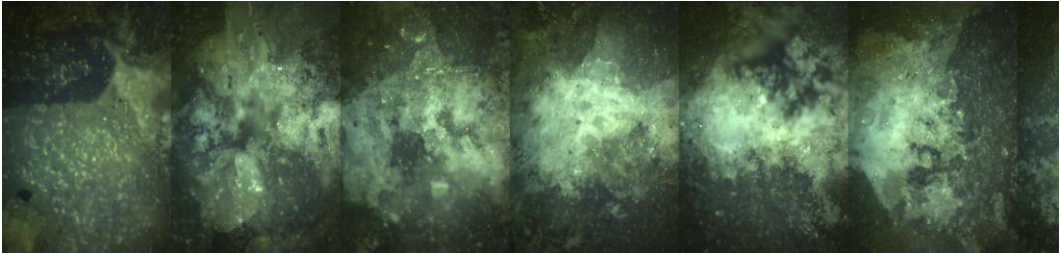
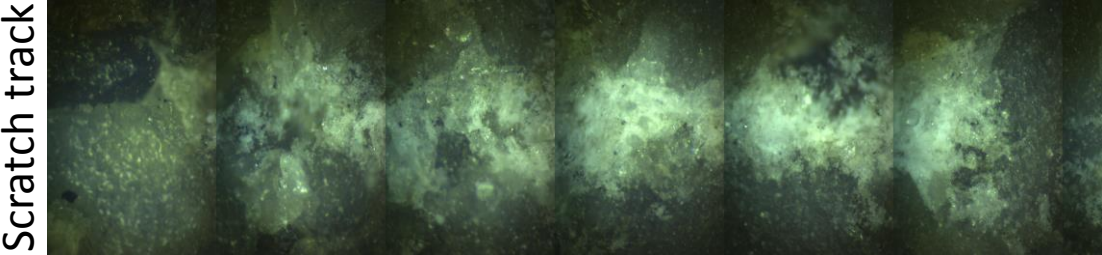
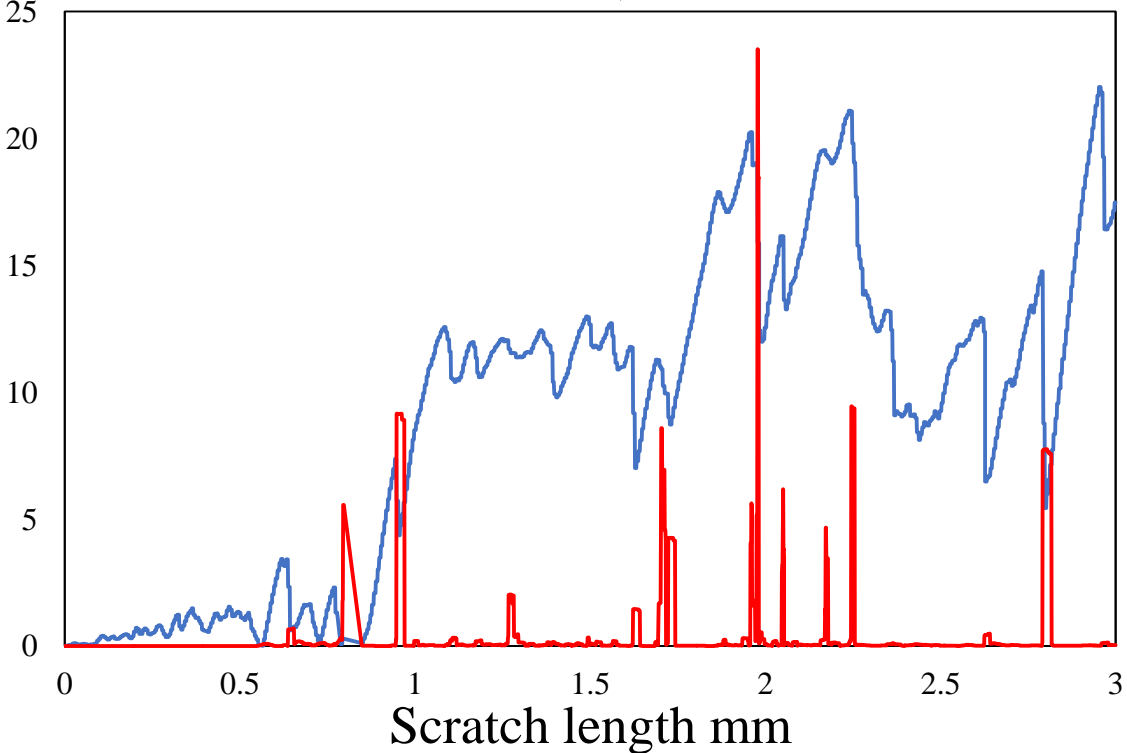
Microscratch

Sandstone

13-14 scratch 3, vertical



13-10 scratch 3, horizontal



Microscale – Fracture toughness

$$\frac{F_T}{K_c d^{3/2}} = 2 \sqrt{\frac{\tan \theta}{\cos \theta}}$$

(Akono et al. *PRL* 2011)

where, $\theta = 60^\circ$, $\frac{d}{R} = 0.132$, $R = 200\mu m$

Average microscale fracture toughness in horizontal and vertical directions before exposure to CO2

Rock type	Well 13-10A		Well 13-14	
	Horizontal	Vertical	Horizontal	Vertical
Sandstone	10.2	7.18	8.23	10.054
Mudrock	14.33	12.06	11.27	9.58

Bi-axial load testing (Core scale)

- Measure sonic velocities -> Calculate elastic moduli at different CO₂ pressures and confinement
- Conducted using Autolab 1500, a multipurpose computer-controlled servo-hydraulic triaxial system



Autolab 1500 unit
(NER Inc.)



Dual purpose core holder assembly (for permeability and sonic velocity measurements), ready to insert into the high pressure vessel



Resistivity heads with a carbonate core between them

Macroscale – Dynamic elastic moduli

Under isotropic assumption,

$$G = \rho_{bulk} V_s^2$$

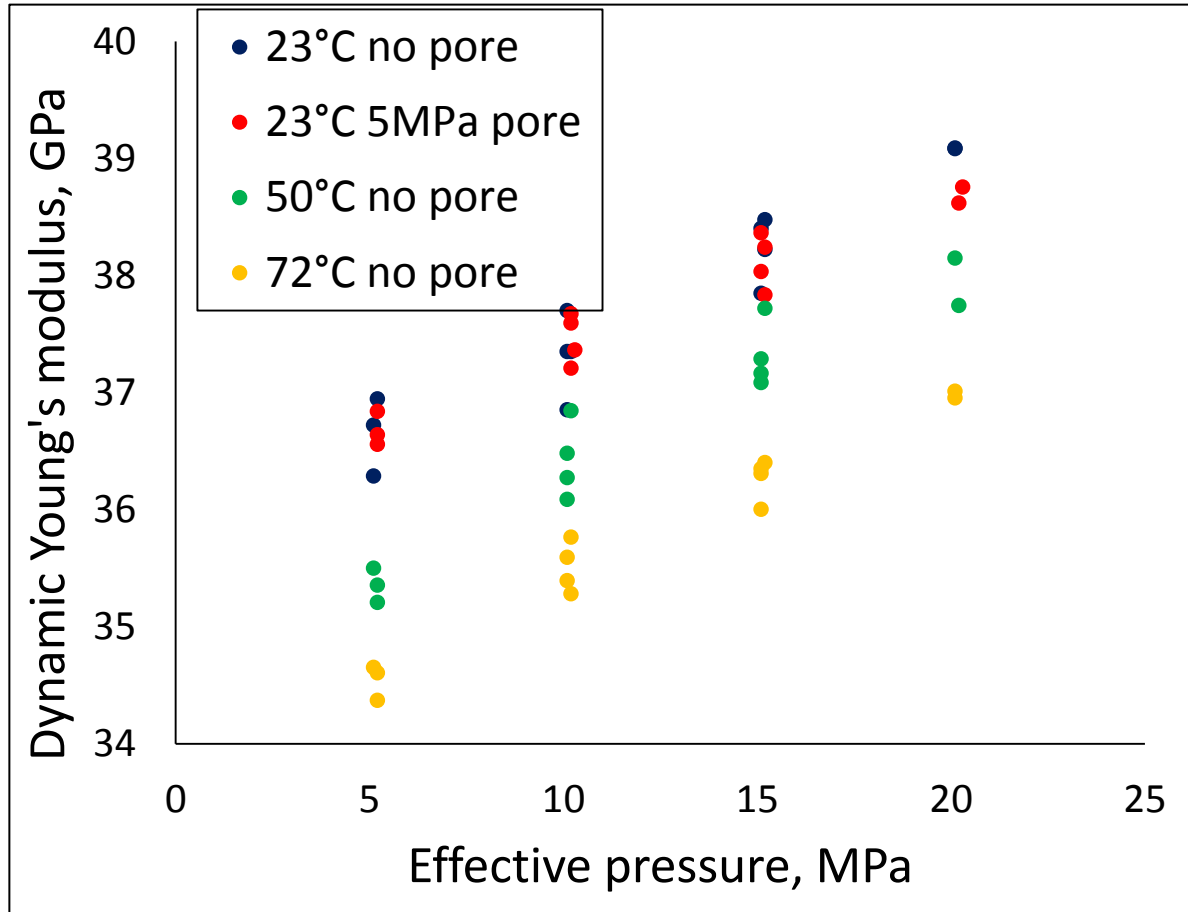
$$K = \rho_{bulk} \left(V_p^2 - \frac{4}{3} V_s^2 \right)$$

$$E = \frac{9KG}{3K + G}$$

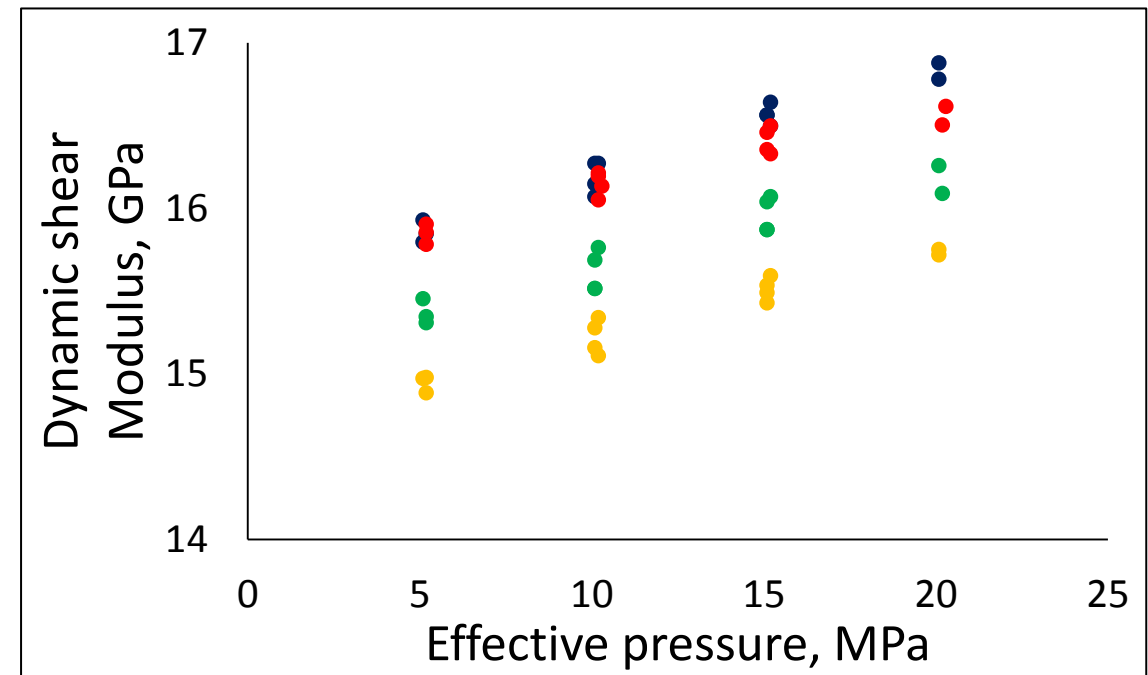
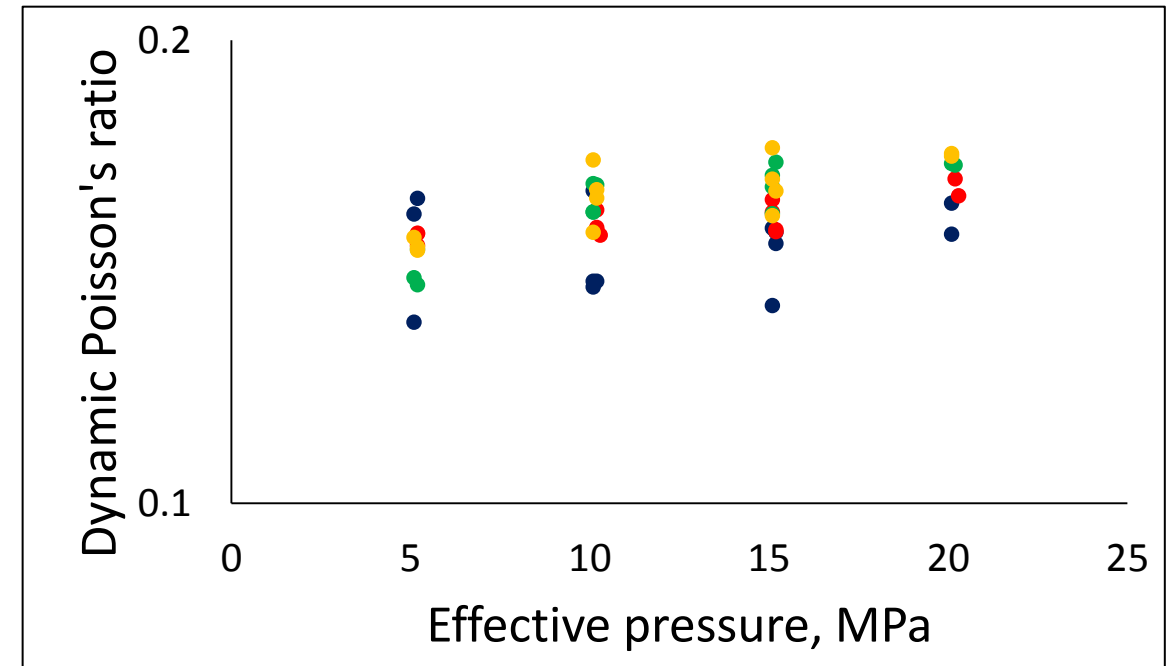
$$\nu = \frac{E}{2G} - 1 = \frac{3K - 2G}{2(3K + G)}$$

where G , K , and E are shear, bulk, and Young's moduli and ν is Poisson's ratio.

Mudrock, Well 13-14

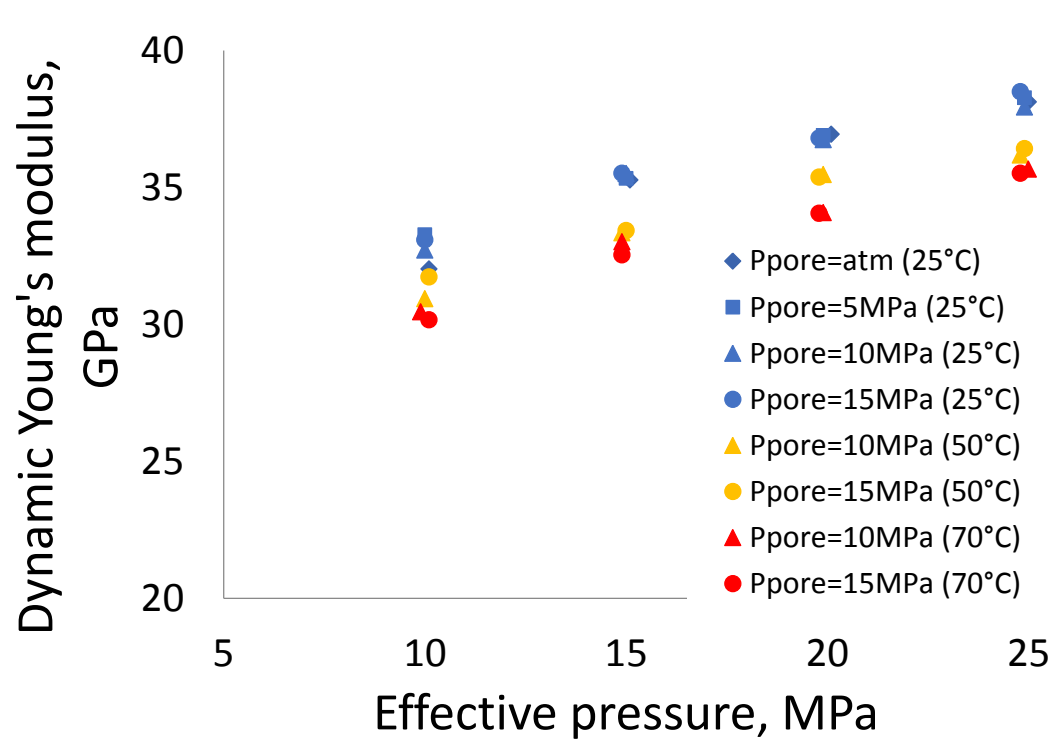


Rock becomes stiffer and stronger with the effective pressure.

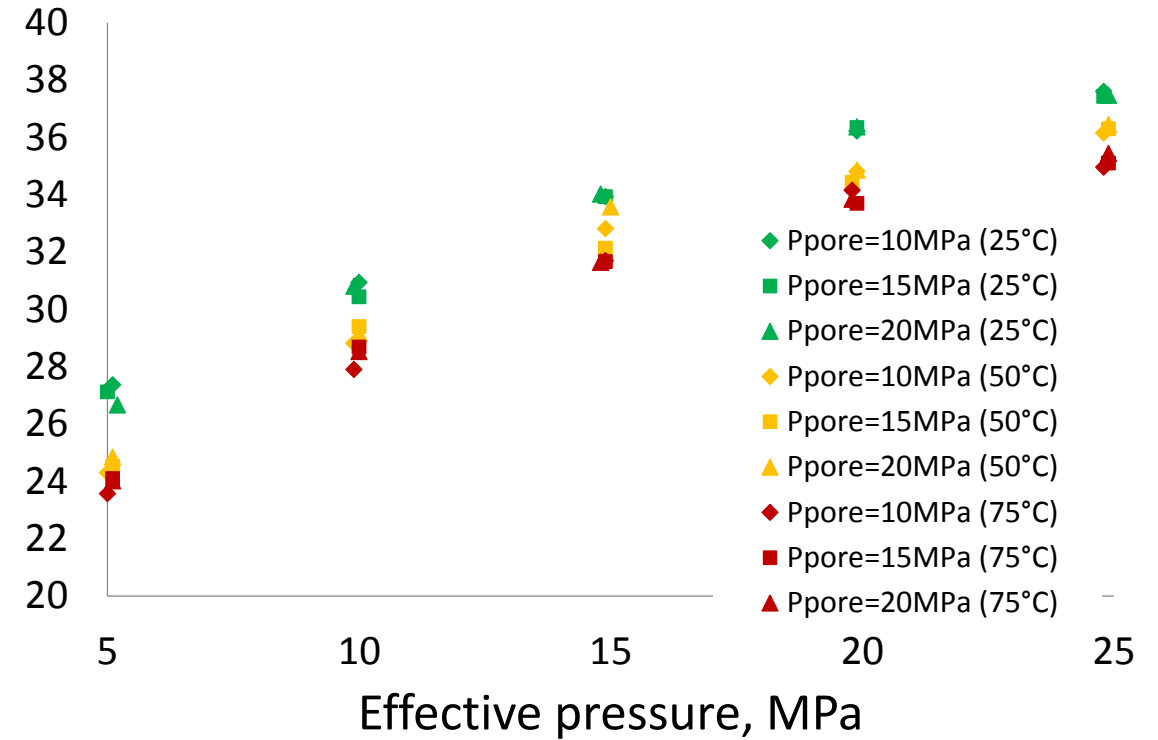


Morrow-B Sandstone

Argon as pore fluid



CO2 as pore fluid



CO2 trend is non-linear. It is not an inert gas.

Effect of pore fluid on porosity and permeability

Before and after CO2 exposure

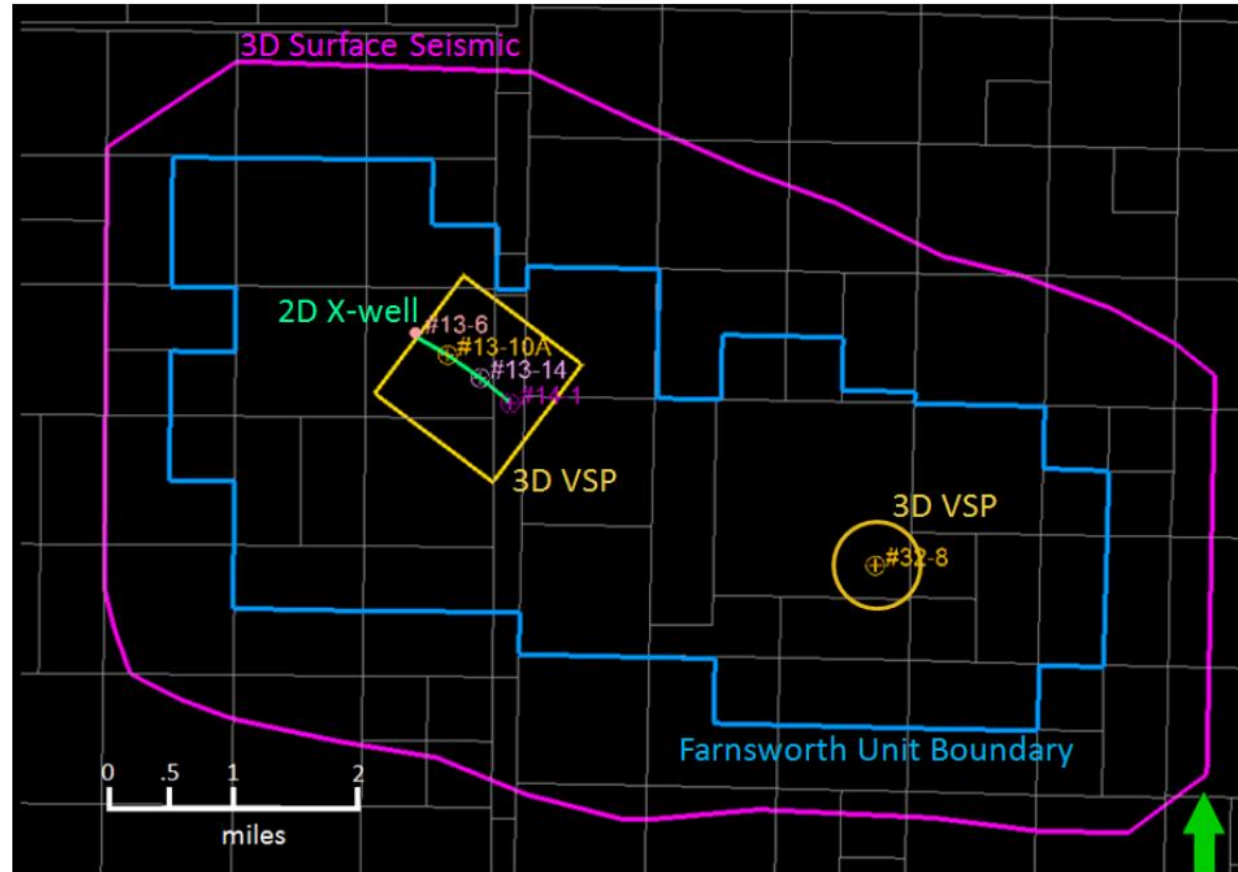
	Pe _{eff} =1,000psi	Pe _{eff} =2,000psi	Pe _{eff} =3,000psi	Porosity, %
SB-SS1 before	8.5 mD	7.9 mD	7.4 mD	13.4
SB-SS1 after	10.0 mD	9.5 mD	9.4 mD	13.4
SB-SS2 before	12.4 mD	11.3 mD	10.9 mD	13.9
SB-SS2 after	15.7 mD	14.9 mD	14.4 mD	14.7

Rock Physics and 4D Seismic Modeling

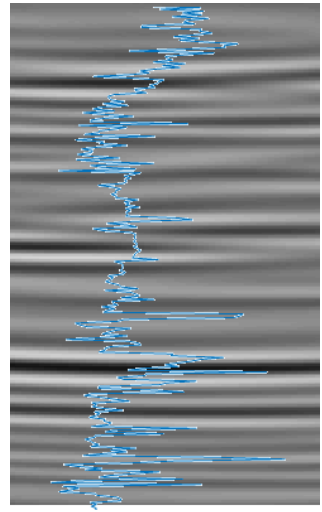
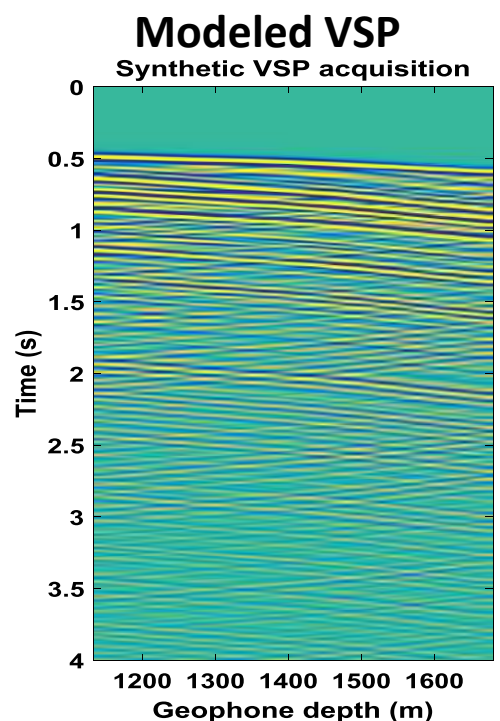
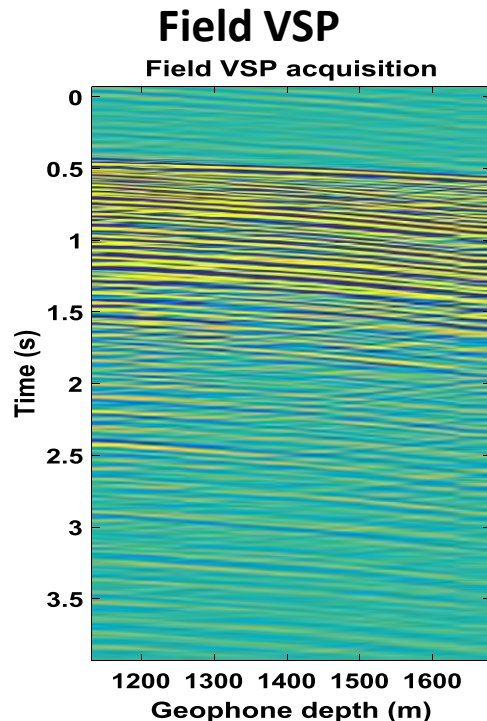
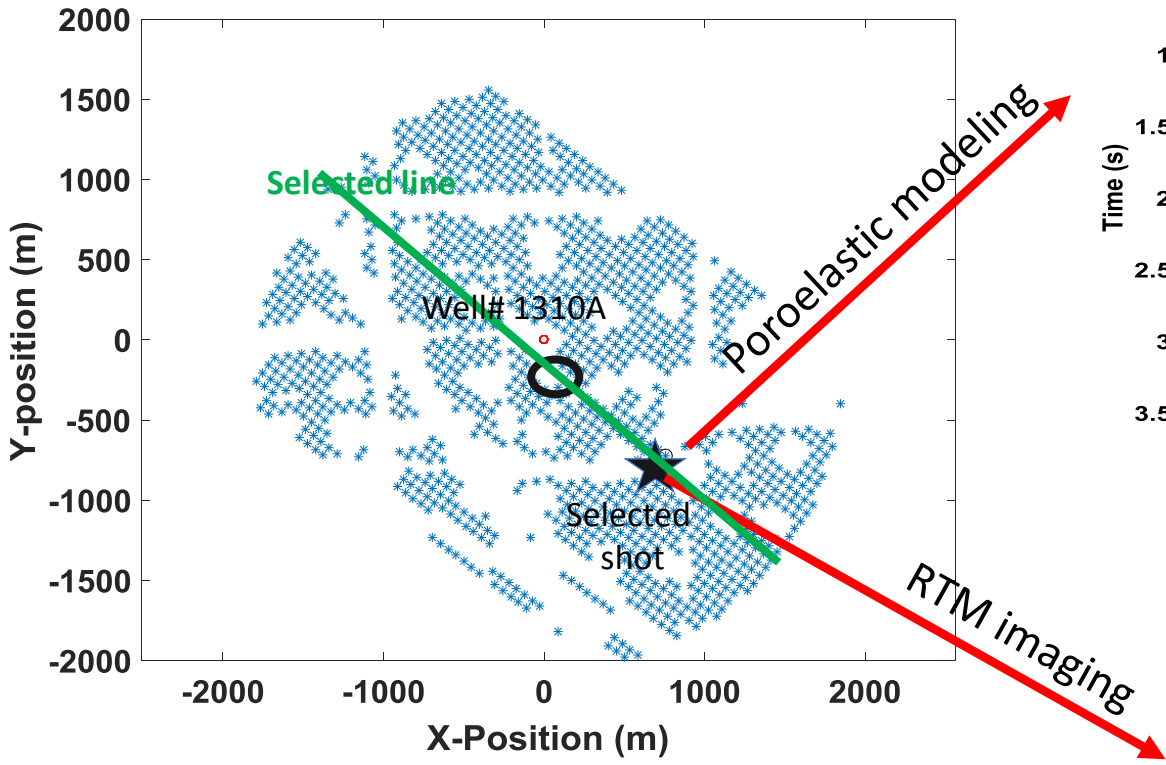
Objective: Derive new seismic imaging techniques for CO₂ monitoring

Available FWU data

- 3D seismic survey conducted in July 2013, survey covers approximately 33 mile² and contains 546 inlines and 369 crosslines, bin sizes were 82.5 ft by 82.5 ft.
- Two checkshot surveys were generated from the vertical seismic profiles (VSP), which were acquired in February 2014 at Wells 13-10A and 32-8

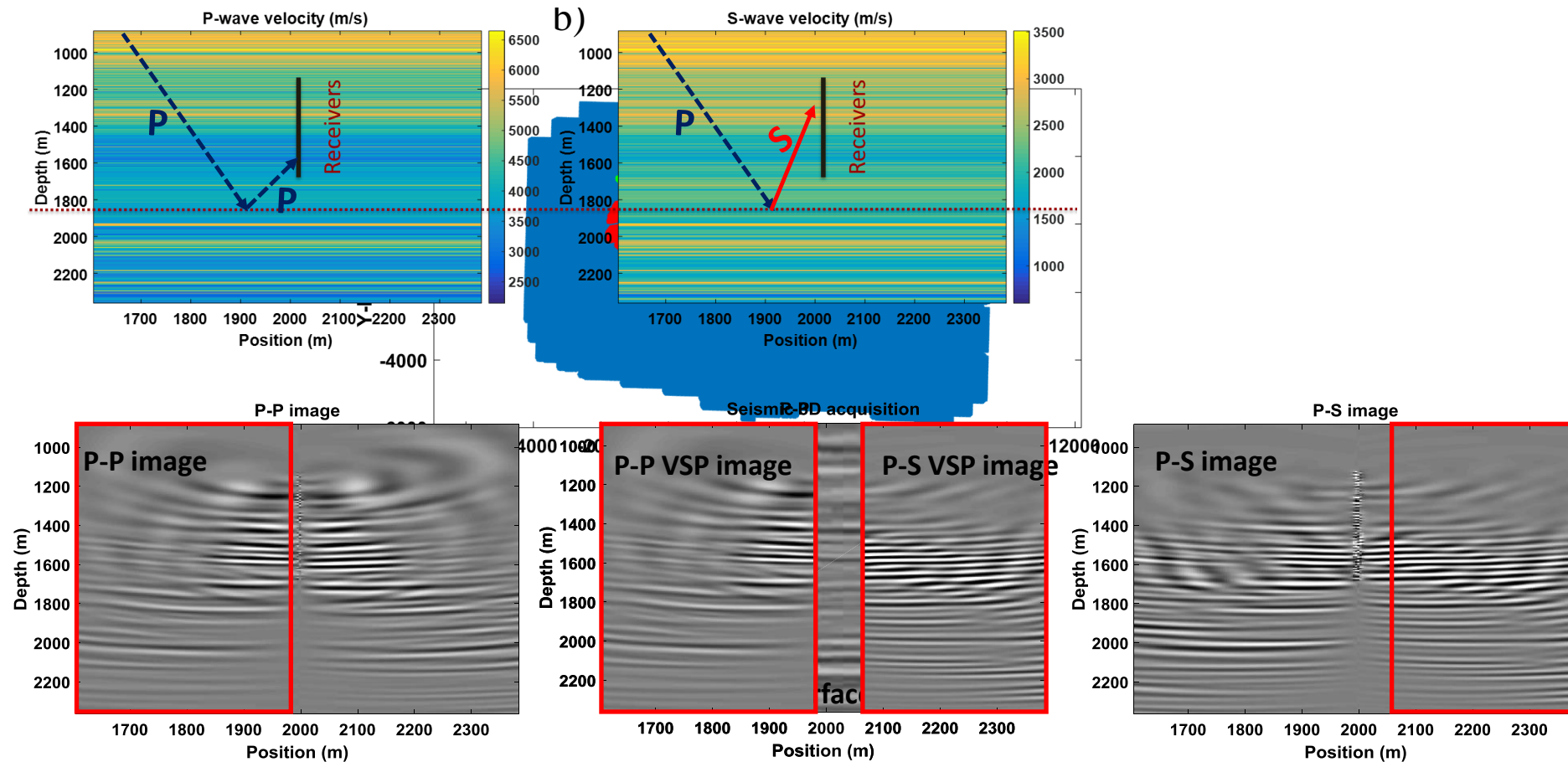


Vertical Seismic Profile (VSP) modeling and RTM imaging



We chose the shot records which are positioned on the selected line. A selected shot record is simulated and compared with the field data.

Validation of 3D VSP RTM Results vs. 3D surface seismic imaging



We perform the multicomponent imaging of VSP data based on separation of the P- and S- waves. In order to validate our result we compared the imaging of P- and S- waves to the imaging of surface seismic data.

4D Rock Physics Analysis

- Use of Gassmann fluid substitution theory to examine the effect of CO₂ injection on the elastic properties

$$\frac{K_{sat}}{K_{matrix} - K_{sat}} = \frac{K_{Dry}}{K_{matrix} - K_{Dry}} + \frac{K_{fl}}{\phi(K_{matrix} - K_{fl})}$$

- Use of Voigt and Reuss method to estimate the matrix bulk modulus and shear modulus

Voigt average

$$M_V = \sum_{i=1}^N f_i M_i$$

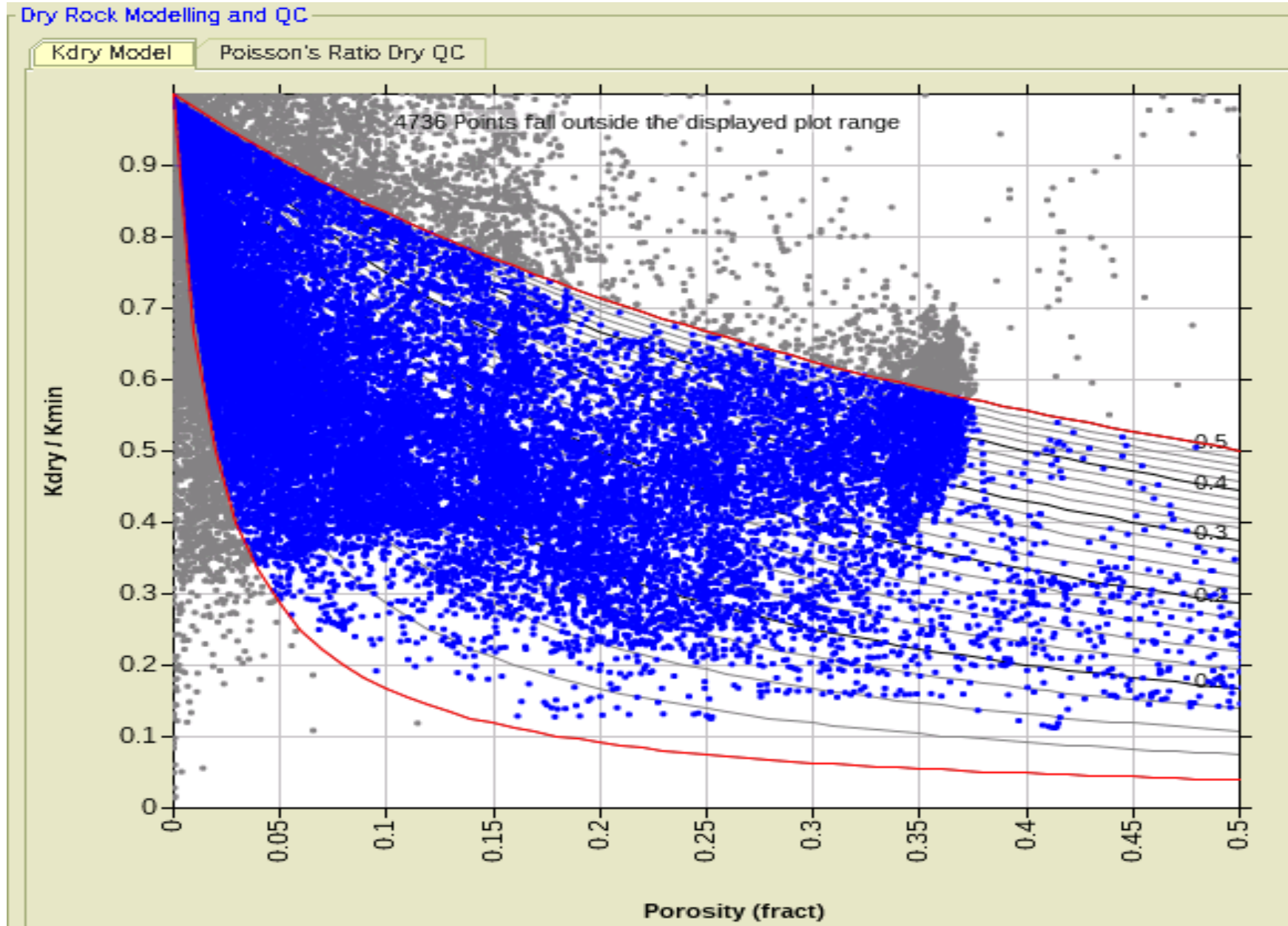
Reuss average

$$\frac{1}{M_R} = \sum_{i=1}^N \frac{f_i}{M_i}$$

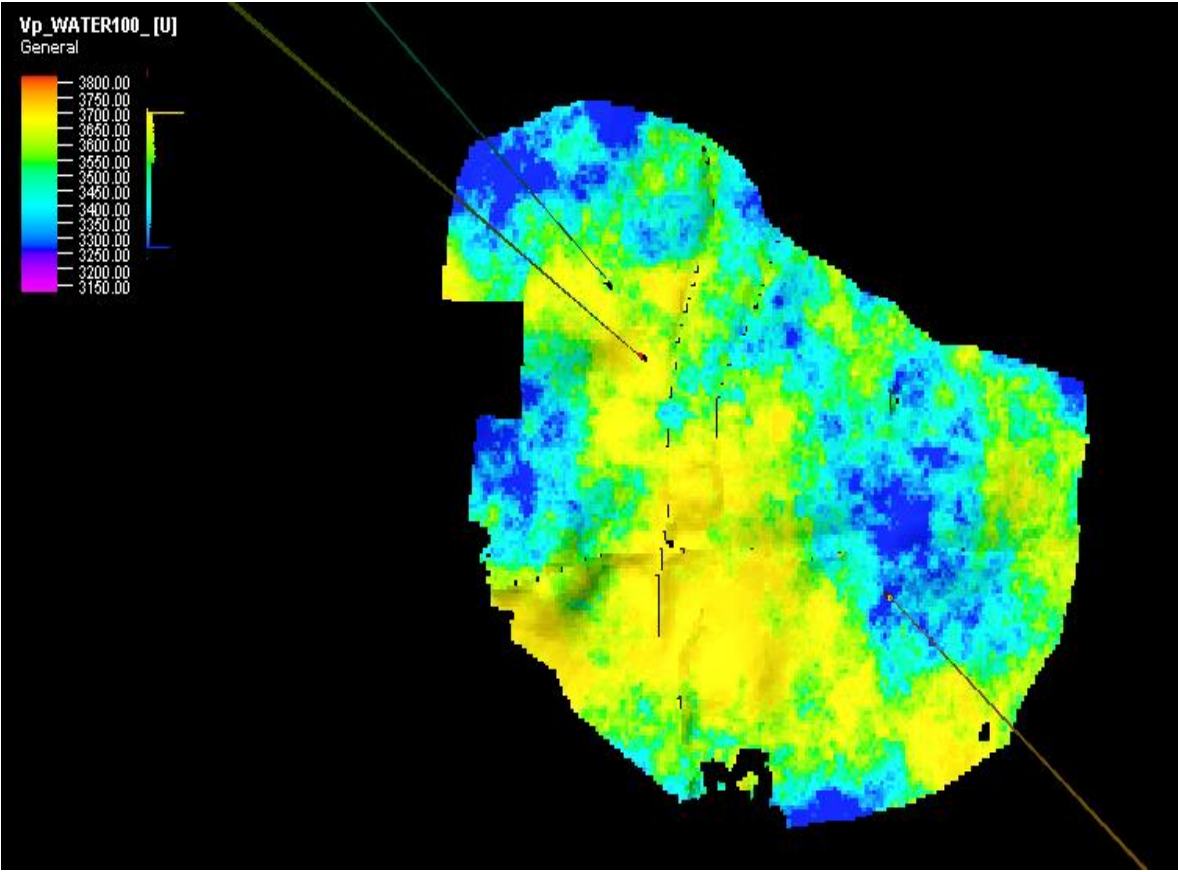
Voigt-Reuss-Hill average

$$M_{VRH} = \frac{M_V + M_R}{2}$$

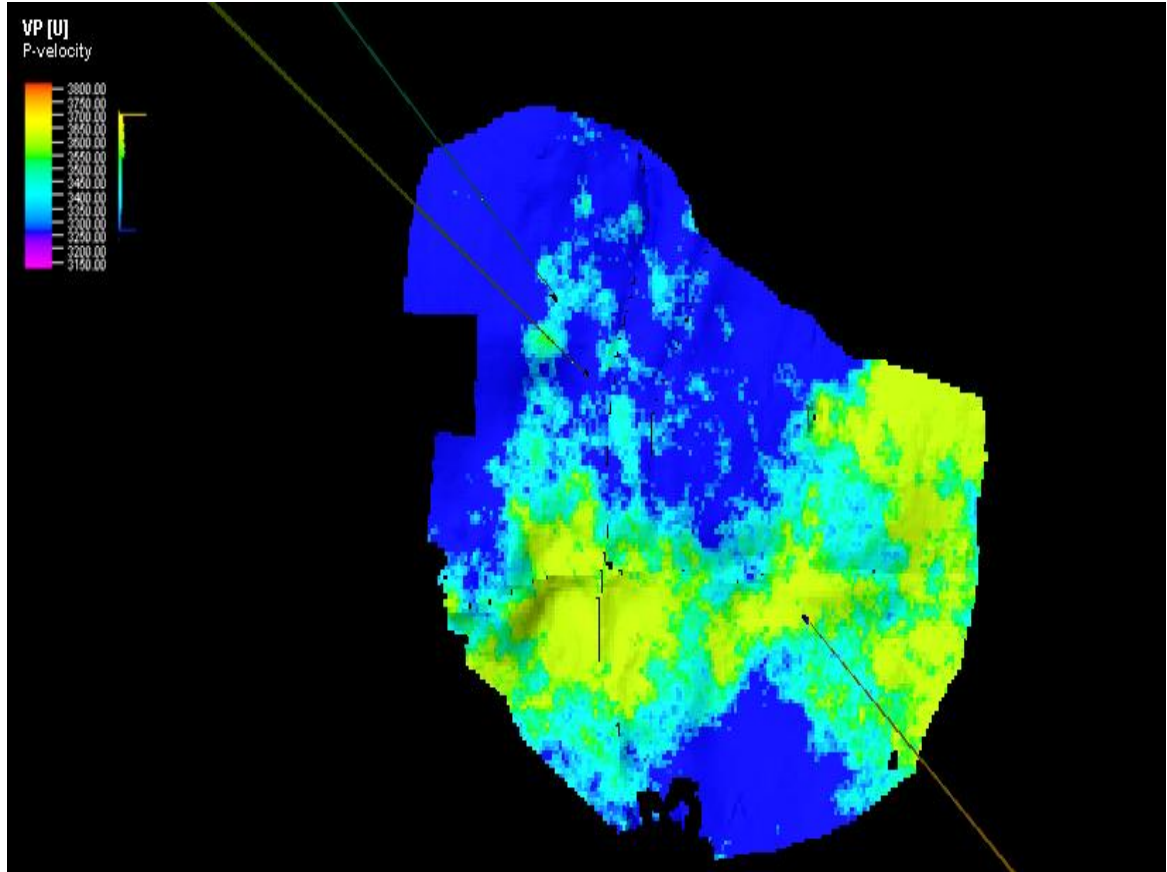
QC of the applicability of Gassmann equation



Changes in Vp, Vs and bulk density due to CO2 injection

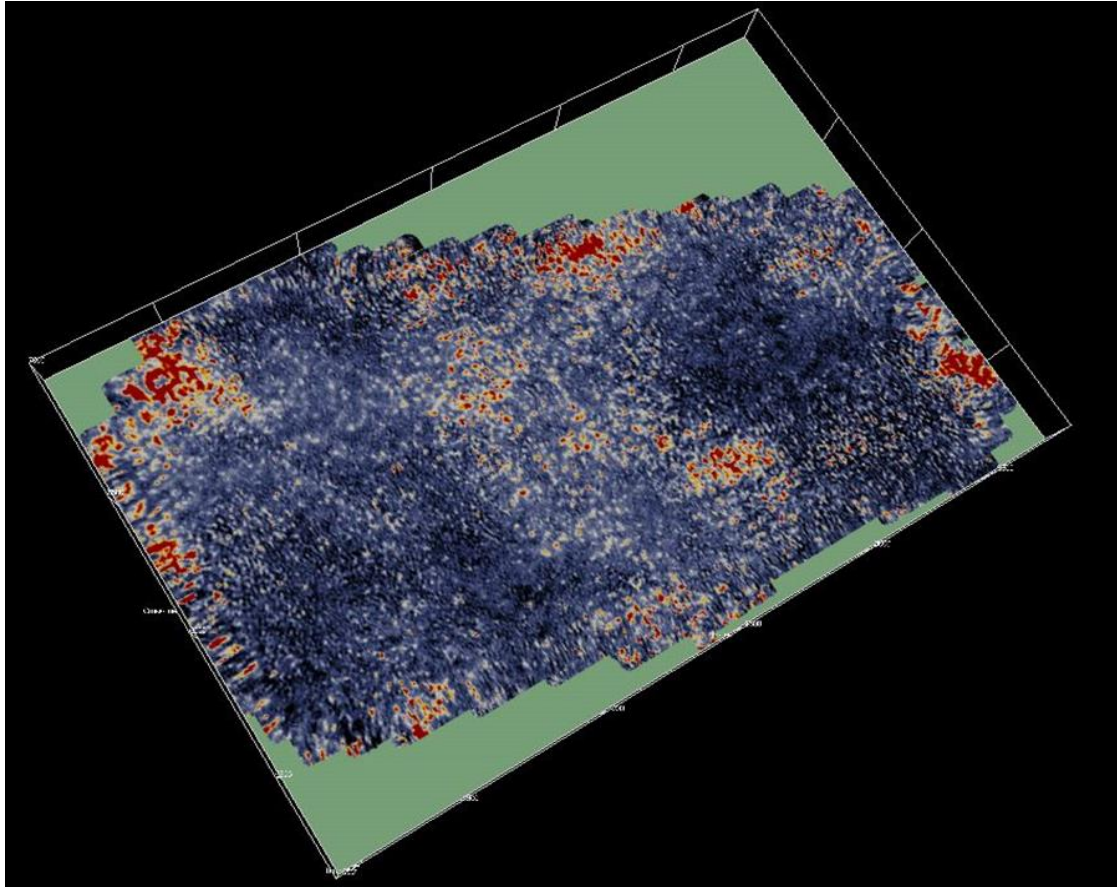


Vp when the reservoir is saturated with water

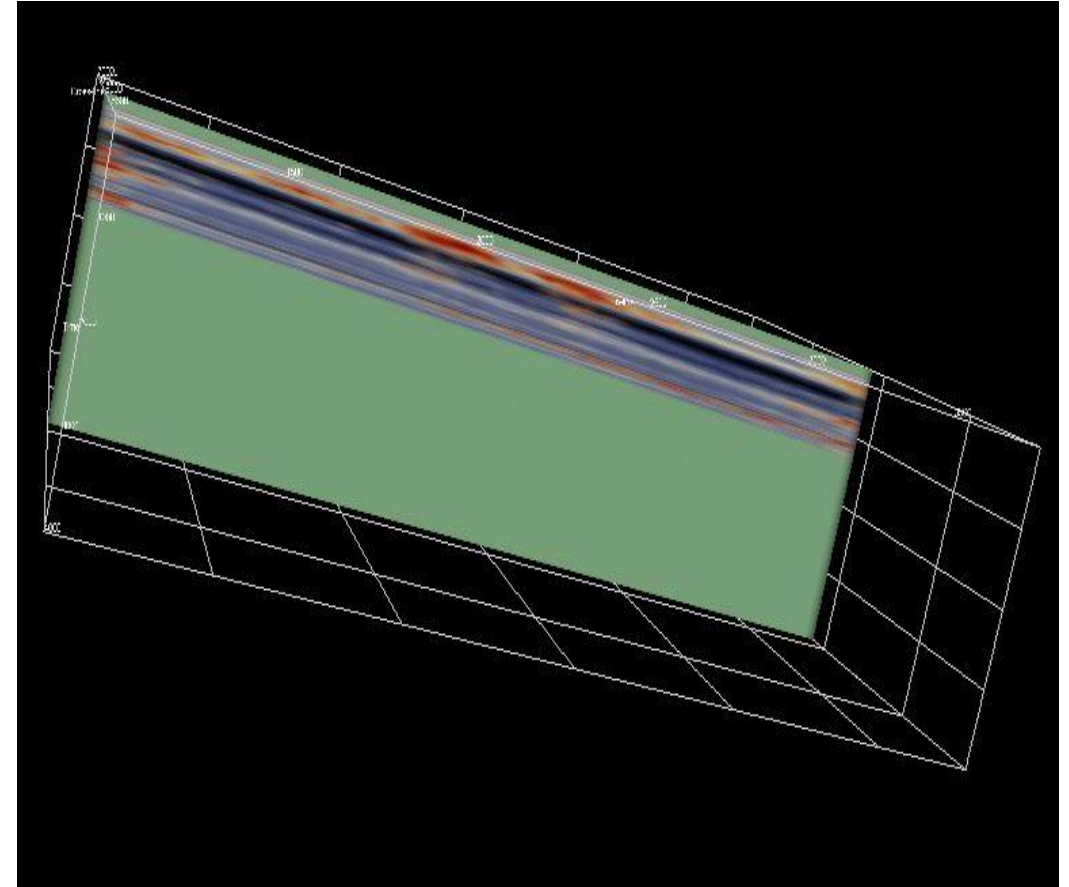


Vp when the reservoir is saturated with CO2

Property Prediction Using Artificial Neural Network

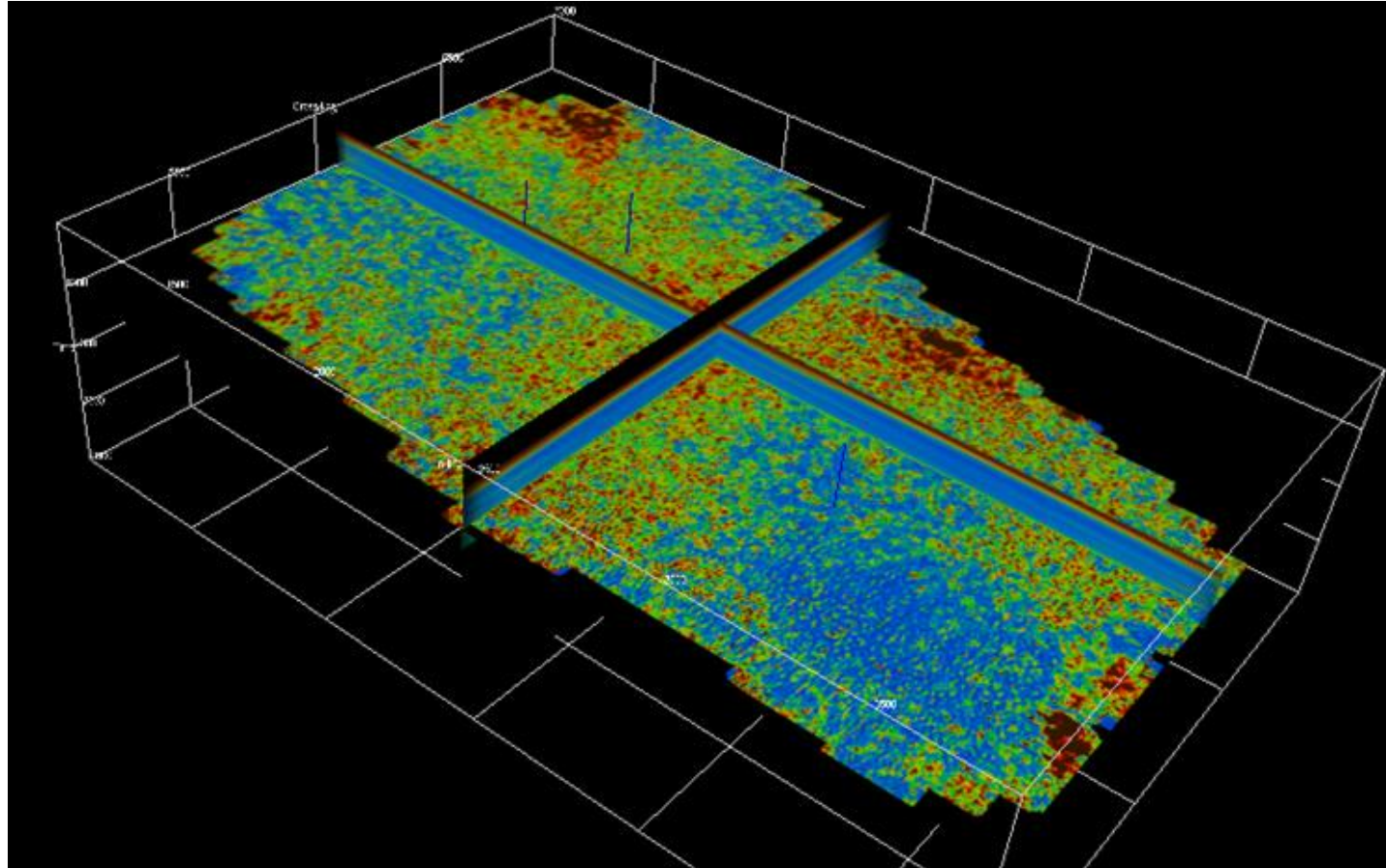


Horizontal (z) slice #1000
Density



Xline #6080 Density

Property Prediction Using Artificial Neural Network

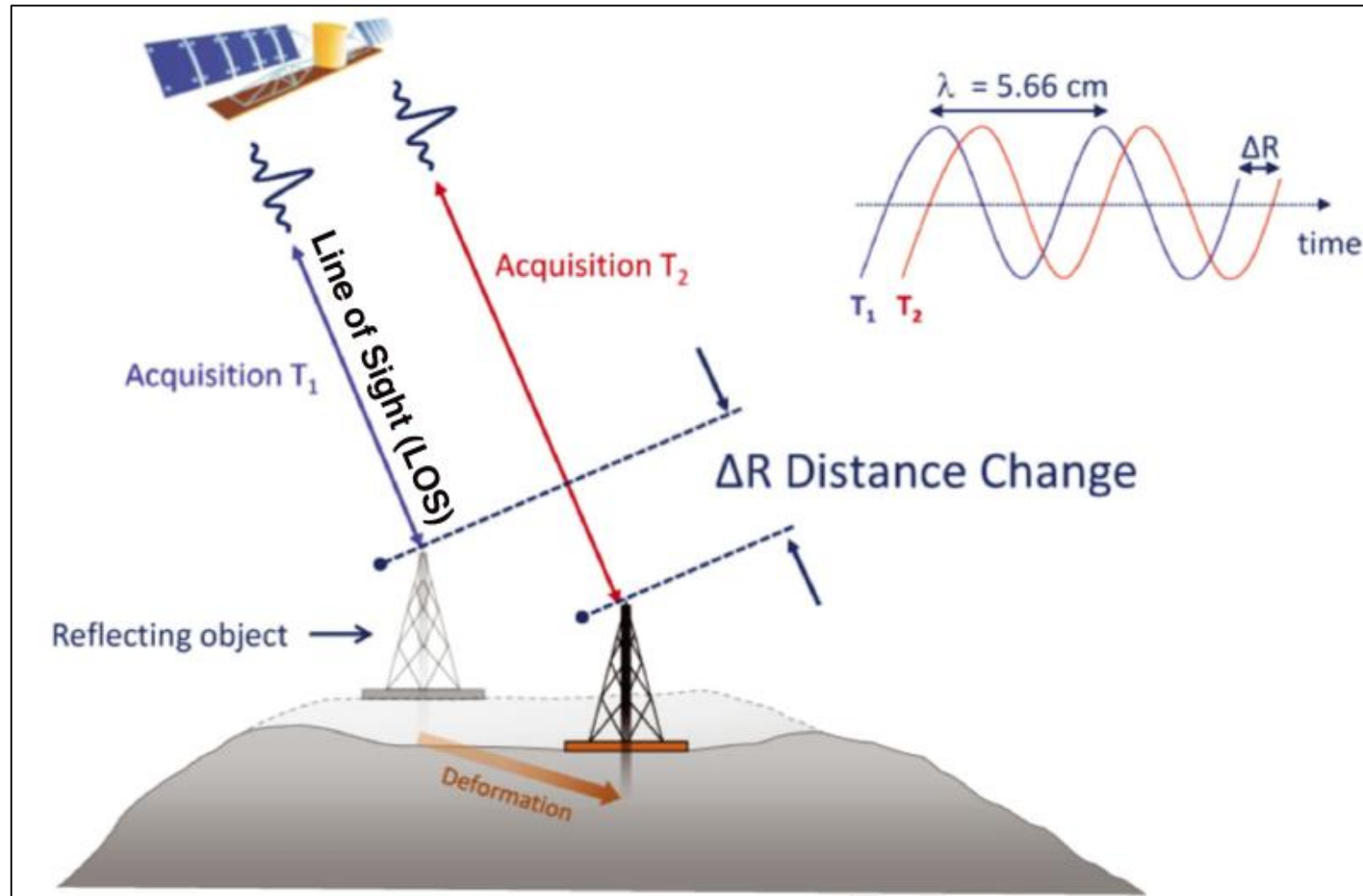


Porosity

Conclusion

- Geomechanical and geophysical modeling approaches are combined to improve the monitoring of mechanical integrity of reservoir and caprock during storage
- The coupled multiphase flow—geomechanical simulation model of FWU can be used to predict changes in pressure, stress, CO₂ saturation, and stress-dependent permeability and elastic moduli.
- RTM imaging technique can image the effect of CO₂ injection. A rock physics model is constructed to account for the effect of CO₂ on elastic properties.
- Geomechanical experiments on FWU cores provided characterization of dynamic elastic moduli with the changes in CO₂ pore pressure. This can be used to determine constitutive model parameters in the simulation model.

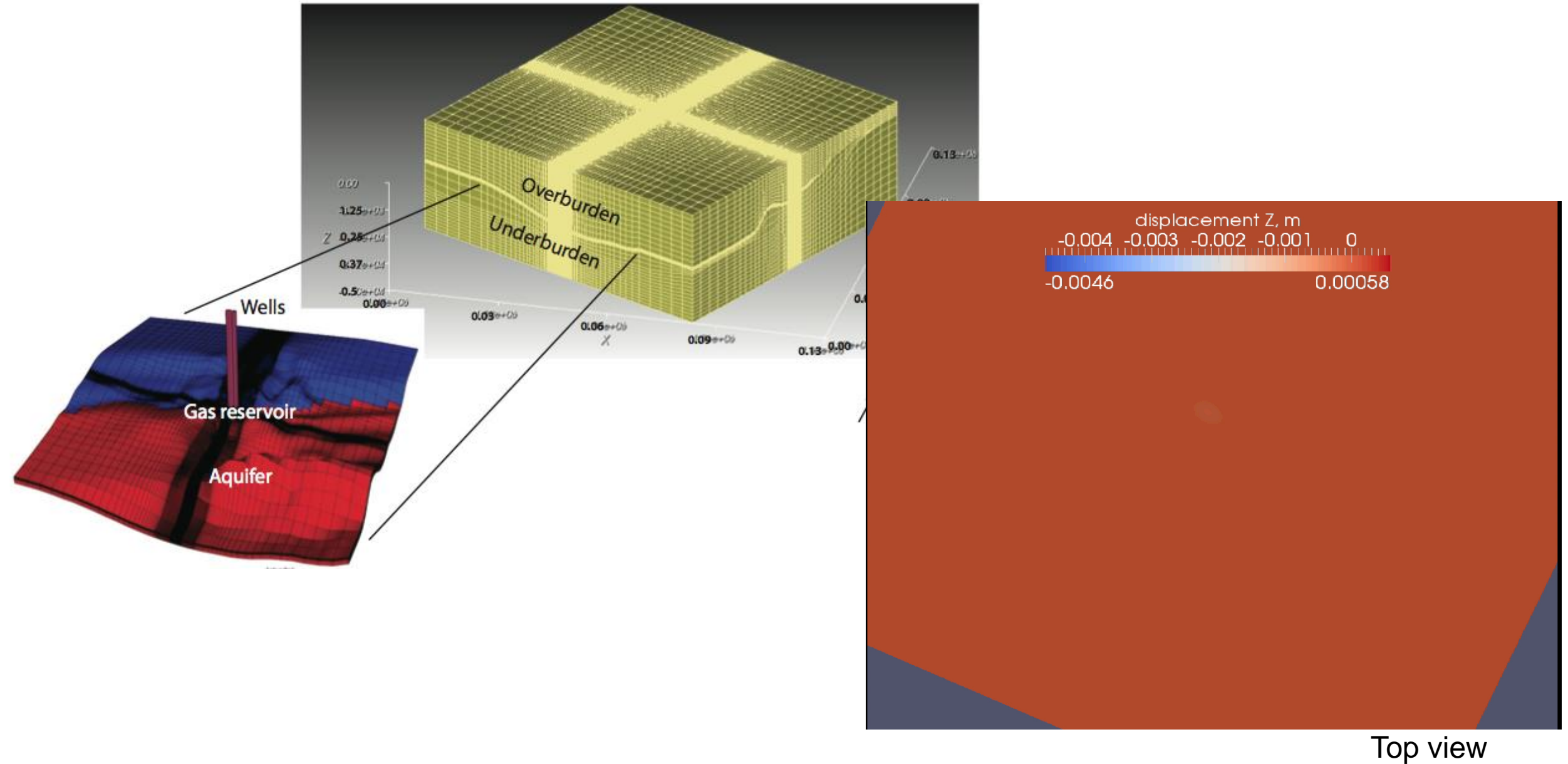
Geodetic Monitoring of Underground Gas Storage (UGS)



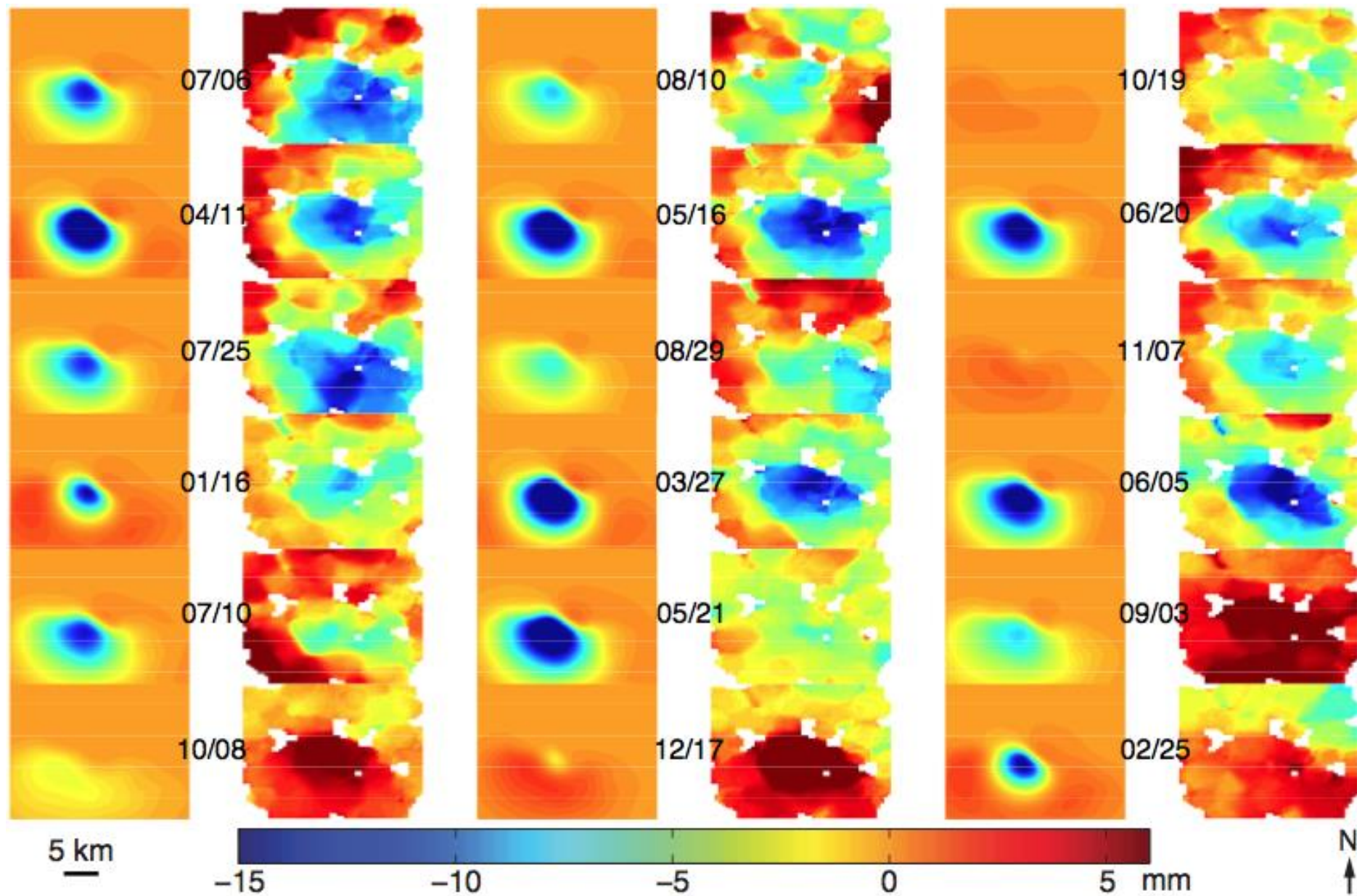
Store in summer, produce in winter.
How much can be stored and how fast?

(Jha et al, Int J Numer Anal Method Geomech 2015)

Finite element modeling and simulation



Compare model results with satellite data



Reduce uncertainty in rock properties

